RED FLUORESCENCE IN BOVINE SERUM ALBUMIN – GOLD COMPLEXES

by

Jacob Michael Dixon

A thesis submitted to the faculty of
The University of North Carolina at Charlotte
in partial fulfillment of the requirements
for the degree of Master of Science in
Applied Physics

Charlotte

2019

Approved by:

_____
Dr. Shunji Egusa

_____
Dr. Donald Jacobs

_____
Dr. Didier Dreau

ABSTRACT

JACOB MICHAEL DIXON. Red Fluorescence in Bovine Serum Albumin – Gold Complexes. (Under the direction of DR. SHUNJI EGUSA)

Bovine serum albumin (BSA)-gold (Au) complexes have been studied in great detail due to their unique red fluorescent (λ_{em} = 640 nm) properties, since being initially described by Xie et al. (*J. Am. Chem. Soc.* **2009**, 131, 888-889) as a Au_{25} nanocluster. We report new findings on these BSA-Au compounds, which were further reducible after synthesis, indicating that these compounds are BSA-cationic Au complexes. We also examined the correlation between pH-induced conformations of BSA and the effect on the resulting red fluorescence to elucidate possible cationic binding sites. The red fluorescence of the BSA-Au complex was associated with only one of five pH-induced isoforms of BSA, the aged (pH > 10) isoform, while the other four BSA conformations (pH < 10) did not result in any red fluorescence. The minimum number of cationic gold per BSA required to yield red fluorescence was less than seven, and internal energy transfer mechanisms could be the reason for the emergence of red fluorescence, based on three-dimensional excitation-emission map measurements. Using various synthesis protocols we determined multiple specific Au binding sites to cysteine disulfide bonds and the N-terminus of the BSA protein. With these findings we present an interpretation of the BSA-Au complex, alternative to the single-site nucleating Au_{25} nanocluster model.

TABLE OF CONTENTS

LIST OF FIGURES

LIST OF ABBREVIATIONS

Å	Angstrom
A-form	Aged form of BSA
Asp	Asparagine
Au	Gold
B-form	Basic form of BSA
BSA	Bovine serum albumin
Cu	Copper
Cys34	Cysteine 34 residue
E-form	Extended form of BSA
EE-map	Excitation-emission map
F-form	Fast form of BSA
kDa	Kilo-Dalton
M	Molar
N-form	Normal form of BSA
NaOH	Sodium hydroxide
NEM	N-ethylmaleimide
Ni	Nickel
Pt	Platinum
TCEP	Tris(2-caroxyethyl)phosphine hydrochloride
TEM	Transmission electron microscopy
UV	Ultra-violet

CHAPTER 1: INTRODUCTION

Initial findings by Xie et al.[1] detail unique fluorescent properties by complexing bovine serum albumin (BSA) and gold (Au). BSA[2-3] is a dynamic and resilient 66.4 kDa transport protein that has five reversible, pH induced, conformational states: "normal" form (N-form) at a pH between 4.3 and 8, "expanded" form (E-form) at a pH less than 2.7, "fast" form (F-form) at a pH between 2.7 and 4.3, "basic" form (B-form) at a pH between 8 and 10, and "aged" form (A-form) at a pH above 10.[4] The protein also contains 66 ultraviolet excitable amino acids in the form of aromatic residues (2 Tryptophan, 20 Tyrosine, 17 Histidine, and 27 Phenylalanine) and 35 cysteines: 34 of which are locked in disulfide configurations. Through the addition of chloroauric acid ($HAuCl_4$) to a solution of BSA and an adjustment of the pH to 12, a red-fluorescent compound is created. This fluorescent compound is suggested to be a Au nanocluster comprising of 25 Au atoms[1] based on the spherical Jellium model.[5] The ensuing reports further describe that the red and blue fluorescence of these BSA-Au compounds is due to Au_{25} and Au_8 nanoclusters, respectively.[6] It has been suggested but not shown that the nucleation sites of these Au(0) nanoclusters is nested within the protein, bound to one of the 17 cysteine disulfide bonds.[1]

Furthermore, the reduction of Au(III) to neutral Au(0) is said to be achieved by tyrosine residues ($pK_{bR} = 10.5$) facilitated in a highly basic reaction condition of pH = 12. In Xie and others work the nucleation sites of Au(0) and Au(III) has not been elucidated and the relation of pH and fluorescence is still not fully understood.[7] While other metal cations such as copper (Cu(II)),[3, 8-9] nickel (Ni(II)),[10] cobalt (Co(II)),[11-12] zinc (Zn(II)),[13-14]

iron (Fe(II)),[15-16] and magnesium (Mg(II))[17] have been studied in detail, no such studies have been completed for Au(III).

1.1 Metal Ions with Serum Albumin

Metals play a crucial role in life processes and it has been increasingly recognized that metals are involved in biological systems for cellular and subcellular functions.[18] The importance of metal ion-protein complexes has also been recognized and one of the most predominate proteins in blood, serum albumin has been known to act as a metal ion scavenger.[19] Human serum albumin (HSA) controls the copper distribution among organs, invariably bound as Cu(II), due to oxidative conditions in the blood.[19] The uptake of Cu(II) by BSA was studied to determine the binding thermodynamics and reversible nature of the binding.[8] In this work Cu(II) was placed in different concentrations in control tubes and allowed to mix with BSA via osmosis. Based on their results, the number of copper ions bound to BSA was estimated to be approximately 6. Interestingly, when using Cu(II)-bound BSA complexes dialyzed against buffer only, some copper ions were resealed from BSA, indicating the reversibility of the binding process of Cu(II) to BSA. Thus the affinity of Cu(II) to BSA was also determined by comparing the binding of Cu(II) to five proteins: α-casein, β-casein, BSA, β-lactoglobulin, and lysozyme.[9] They determined that the free energy of binding of Cu(II) to BSA in acetate buffer was -6.5 kcal/mol, and that the binding affinity of Cu(II) changes based on the concentration of free Cu(II) and the temperature of solution.

While nickel has not been shown to be an essential metal in humans it is essential for plants and microorganisms. For humans and mammals in general, nickel is a toxic element, mainly as Ni(II) which is known to act as a strong allergen.[20] Thus, the removal

of Ni(II) in the body is done mainly by blood albumins.[21] The number of bound Ni(II) ions to BSA was measured by looking at the electrophoretic ability of BSA based on the concentration of Ni(II).[10] The results showed that the number of available binding sites in BSA for Ni(II) was around 16, and that the binding sites were imidazole groups located on the surface of BSA. Binding of Ni(II) to BSA in the presence of 5 M urea was also conducted, which is known to disrupt the helical structures of protein. A greater number of binding sites where observed, indicating that the Ni(II) also has an affinity for carboxyl, albeit the affinity of Ni(II) to carboxyl groups was much lower than that of the imidazole groups.

Cobalt is an essential element for humans in the form of cobalamin, or coenzyme B12. Humans are mainly exposed to ionic cobalt (Co(II)) from normal nutrition, such as Co(II) in yeast or Co(II) from environmental exposure.[22] It was initially thought that the primary binding site of Co(II) was the N-terminus as previously found for Cu(II) and Ni(II)[23], and studies of the binding affinity of Co(II) to BSA were very low.[11] However, two addition binding sites, using Co(II), were determined.[24-25] These sites, found in HSA, include metal binding site (MBS) site A, which involves the cationic cobalt binding to His67 and MBS site B which has not been determined, but is known not to involve His39.[26]

Zinc plays a vital role in mammals by helping the immune system fight off bacteria and viruses and is used in the synthesis of proteins and DNA. All functions of zinc are performed by Zn(II), the only stable oxidation state of zinc compounds. The binding site of Zn(II) was found using a competitive binding study against Cu(II).[27] Zn(II) was able to replace Cu(II) at MBS site A. While this binding site has been found in HSA, comprised of His67, Asn99, His247, and Asp249, it has not been confirmed yet in BSA. Though as

those same amino acid residues would have to be His67, Asn98, His246, and Asp248 in BSA. It also was found that Zn(II) was bound to MBS site B, the undetermined binding site, with lower affinity than MBS site A.[28]

The most important role of iron in body is to act as a dioxygen carrier in hemoglobin.[29] It is present as Fe(II) or as Fe(III) when in the resting state of some enzymes, depending on function. In the blood, iron is oxidized to Fe(III), which is its most stable form when in the presence of free oxygen.[30] Under normal conditions in the blood, albumin most likely is not binding Fe(II). Though it was found *in vitro* that HSA will bind the ion under very high iron concentrations.[31] Studies performed found that the Fe(II) binds non-specifically and binding at any of the known binding sites does not seem to occur. The binding of iron in BSA was also found to occur with protein digestion products and the carboxyl groups were identified as the site of complexation.[15]

Overall, four common binding sites have been found for various metal ions, including Cys34, the Asp-fragment (Asp1-Thr2-His3)"[8-10], His67 binding site, and a fourth undetermined location. Metals also seem to have the ability to non-specially bind to albumin as in the case of Fe(II) and Ni(II). In all these findings, no evidence of nanoparticle formation has been observed for these metal cations. Moreover, the reasons for the suppression of the intrinsic UV fluorescence of BSA (λ_{em} = 340 at pH = 7) is still unknown.[32-33] This thesis will aim at elucidating the binding location or locations of Au(III) based on pH conformational changes in BSA using various synthesis procedures and spectroscopy. In addition, it will propose an interpretation of the fluorescence of the BSA-Au compound alternative to the single-site nucleation of a neutral Au_{25} nanocluster.

CHAPTER 2: BACKGROUND OF STUDY

Noble metal nanoclusters are in a unique, intermediate state between single atoms and bulk metals. These nanoclusters carry with them, intriguing properties and contain a vast potential for applications in various fields, though none seem more previously studied than Au_{25}.[34] First synthesized in 1998,[35] and then structurally determined in 2008,[36] Au_{25} has been of great interest due to its easy preparation,[37-40] high stability,[36, 41] and easy functionalization.[42-45] Due to its large presence in the nanoscience field during this time, a new protocol in synthesizing this nanocluster has high impact.

The initial report by Xie et al. describes a simple, 'green' synthetic route for forming Au_{25} nanoclusters using a commonly available protein, bovine serum albumin and chloroauric acid. The evidence supporting nanocluster formation was based on a single experimental finding and a proposed mechanism of nanocluster formation. Xie et al. used matrix-assisted laser desorption ionization time-of-flight (MALDI-TOF) mass spectrometry, in which a matrix-bound molecule is ionized and fragmented by high-energy laser radiation. The fragmented particles fly through a vacuum with an electric field and the time of flight for each fragment is recorded. The recorded flight times of each fragment can then be analyzed to give a molecular weight of the original molecule. Using this experimental procedure, Xie et al. found a 5 kilo Dalton (kDa) difference in the mass of BSA and BSA complexed with gold; thus this difference was attributed to 25 Au atoms (Au = 196.966 u). Using these results a theory of nanocluster formation was developed using the spherical Jellium model, tyrosine residue reduction, and cysteine disulfide nucleation growth.

The spherical Jellium model[5] is a theoretical model that predicts the emission energy in electron volts (eV) of a Au nanocluster in the regime of 1 to 30 Au atoms. This model shows that for clusters of this size, the emission energy will fall somewhere in the visible light spectrum. The results of Xie et al. found that after synthesizing the BSA-Au complex a red fluorescence (λ_{em} = 645) appeared when excited in the UV (λ_{ex} = 365). Thus by comparing the emission energy of the BSA-Au complex to the spherical Jellium model, the theoretical nanocluster that could produce λ_{em} = 645 was closest to a Au_{25} nanocluster.

Chloroauric acid when dissolved in water will yield cationic Au(III) in solution, thus in order to form a neutral Au_{25} nanocluster Au(III) must be reduced to Au(0). The mechanism to reduce Au(III) to Au(I) is well known and involves aromatic residues as the reducing agent.[46-49] Certain amino acid residues have the capacity to act as reducing agents when the pKa of the R-group on the amino acid is above a specific value. Xie et al. determined that as red fluorescence occurs when the pH is brought above 12 then tyrosine must act as the reducing agent because the reduction potential of tyrosine is activated when the pH is brought above 11.5.

Finally, the nucleation site of Au_{25} was proposed to be at one of the 17 disulfide bonds throughout the protein. It is well documented that Au has a high affinity for cysteine and thiol in general, and that the binding energy of a Au-thiol bond is very high.[50-51] Thus, nucleation of this nanocluster occurs at a cysteine disulfide bond and the existence of Au_{25} is supported by the Jellium model, tyrosine reduction, and MALDI-TOF spectroscopy. The reports that followed perpetuated this hypothesis and continued to advance nanocluster science.[6] However, the overwhelming support that these metal-protein compounds are in

fact neutral nanoclusters facilitated inside hydrophobic regions of the protein-space has not been confirmed, and the overall fluorophore mechanism has not been elucidated.

Understanding the origin and mechanism of red fluorescence specifically in these BSA-Au compounds is fundamental in order to fully utilize this fluorophore in a variety of ways. While some studies provide insight into the Au binding sites in BSA's native conformation,[33, 52] no information is provided in BSA's other four conformational states.

The Jellium model is used initially by Xie et al. as it describes well the fluorescent emission of a small Au nanocluster, though if this model was to be correctly applied, a Au_{25} nanocluster should emit beyond 760 nm, farther into the IR. The Jellium model is also based on a theoretically perfect sphere of Au though reports from the same time showed that a Au_{25} nanocluster is more likely a very complex structure of 25 Au and 18 SH commonly denoted as $Au_{25}(SR)_{18}$.[34] In order to form this nanocluster in BSA, nucleation would have to involve 9 different disulfide bonds throughout the protein molecule. While the evidence of metal reduction by aromatic residues is known, it must first be found at exactly what pH the red fluorescence emerges.

BSA has five unique conformational states based on pH and in order for a nanocluster to nucleate to a cysteine disulfide bond, which is buried inside the hydrophobic pockets of the protein, the protein must unfold to allow ions of Au inside. It is important to determine if red fluorescence is emerging due to the reduction of cationic Au above a pH of 12, or if the fluorescence is emerging at one of the conformational transition points at pH = 10 or pH = 8. Finally, BSA has many important functions in the blood, one of which is as a scavenger of metal ions. Thus, BSA has binding sites capable of holding metal ions, so it is important to determine where Au is binding and if the emergence of red fluorescence

is due to cysteine thiol binding or another surface-bound binding site on the protein molecule. While the current hypothesis is widely accepted, few key questions must still be addressed to confirm or negate the existence of a Au_{25} nanocluster.

The current evidence presented does not lend itself to support a Au_{25} nanocluster and may be more aptly labeled as a BSA-Au compound. Thus, there is need for a better understanding of these BSA-Au compounds and what leads to the formation of its unique fluorescence. It is also important to elucidate the binding site or sites for Au in the protein to have a better understanding of the fluorescence mechanics, and to see what effect different pH values have, and what pH is required for fluorescence to occur. The long term goal of this research is to determine the binding site or sites of Au(III) that produces red fluorescence and develop an understanding of the mechanism involved.

In this current study, the objective is to provide evidence that the red fluorescence of this metal-protein compound is due to the interaction of Au within a local site in BSA and not due to the formation of a neutral Au_{25} nanocluster. Thus, a few key questions must be answered, which is first to analyze the reducibility of these BSA-Au compounds, and to determine if all the bound cationic Au has been reduced. Second, the parameters that allow for the formation of red fluorescence must be elucidated, including the pH at which red fluorescence occurs and the stoichiometric ratio of BSA to Au that facilitates fluorescence. Lastly, the potential binding site or sites of Au must be found and the effect that each binding site has on red fluorescence emergence must be determined.

The results of this study will be valuable in forming the fundamental understanding of this metal-protein compound and its unique optical properties. It is important to fully understand these unique optical properties and large stokes shift before these procedures

can be applied to more systems. Understanding of this system could also be used in discerning similar metal-protein compounds with these optical properties and could be applied in applications such as imaging[22-24] and nanomedicine.[25-30]

CHAPTER 3: MATERIALS AND METHODOLOGY

3.1 Materials and Characterization

All chemicals, including bovine serum albumin (BSA, 96 %) gold (III) chloride trihydrate (chloroauric acid, $HAuCl_4 \cdot 3H_2O$, 99.9 %), copper (II) chloride dihydrate ($CuCl_2 \cdot 2H_2O$, 99.999 %), nickel (II) chloride hexahydrate ($NiCI_2 \cdot 6H_2O$, 99.9 %), sodium borohydride ($NaBH_4$ 99.99 %), *N*-ethylmaleimide (NEM, > 99.0 %), tris(2-caroxyethyl)phosphine hydrochloride (TCEP, > 98.0 %) were obtained from Sigma-Aldrich and were used as received. HPLC-grade water was obtained from Millipore and used without further purification.

The primary research method for this study is metal-protein compound synthesis and spectroscopic analysis. In order to answer the problems expressed, multiple synthesis procedures will be followed and these as synthesized compounds will be analyzed using fluorescence and absorption spectroscopy. Fluorescence spectroscopy and excitation-scanned spectroscopy (excitation−emission mapping) were performed with an Agilent Cary Eclipse or Horiba Fluoromax-4 fluorescence spectrophotometer. For excitation−emission mapping, the samples were excited with 5 nm intervals in wavelength, and their emissions were recorded using 2 nm increments. Ultraviolet−visible (UV−vis) spectra were collected using a Shimadzu UV1800 spectrophotometer with 0.5 nm increments in wavelength.

3.2 Methodology

Synthesis of the BSA-Au compounds as first described by Xie et al. is as follows: The compound is prepared via two different protocols at 37 °C. Protocol (1): 1 mL of

HAuCl4 aqueous solution (10 mM) is added to 1 mL of aqueous BSA (0.75 mM, or 50 mg/mL), according to Xie et al. The two solutions were combined under vigorous stirring at 750 rpm. Upon addition of the HAuCl4 solution to the BSA solution, the color changed from clear to light yellow, and the pH of the solution is 3.0. After 2 min, 1 M NaOH is added to achieve the pH of 12, or to the desired pH. The color is observed to transform from yellow to dark yellow after 12 hours and from dark yellow to brown after 48 hours, at which time red fluorescence is recorded under $\lambda = 365$ nm excitation (**Figure 1)**. This red fluorescence is stated to originate from a neutral Au_{25} nanocluster, in which 25 Au atoms are reduced by aromatic residues in the protein from Au(III) to Au(0).

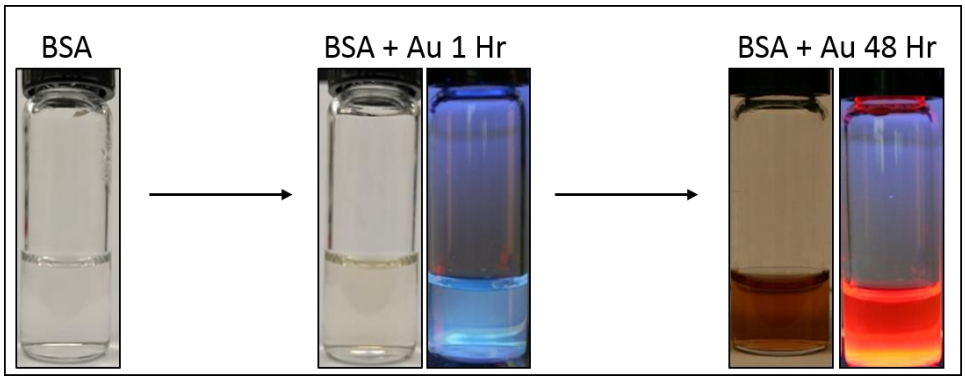

Figure 1. Synthesis procedure of the BSA-Au compound. After 1 hour the sample is light yellow and the fluorescence is unaltered. At 48 hours the sample is now brown and red fluorescent under UV excitation.

Protocol (2): 1 mL HAuCl4 aqueous solution (10 mM) is added to achieve the pH of 12, or the desired pH, and is added to 1 mL of aqueous BSA (0.75 mM), also adjusted to the same pH, under vigorous stirring at 750 rpm. The reaction proceeded for 2 h, then the solution is stored at room temperature. After 48 hours the solution is also observed to transform from yellow, to dark yellow, to brown and the same red fluorescence is observed when excited with UV ($\lambda = 365$ nm) light. BSA−Au compounds were purified and were

filtered through 30 kDa membrane filters (Amicon Ultra, Milipore) by repeated centrifugations at 4000 rpm to remove excess reactants.

After synthesizing these BSA-Au compounds, the formation of Au(0) can be confirmed using sodium borohydride to reduce any leftover cationic Au. The sample is first purified through centrifugation, removing all unused reactants. Using the as-prepared and purified BSA-Au compound sodium hydroxide is prepared at 0^{o}C and reacted with the BSA-Au compound. If reduction does occur then this will indicated the presence of protein-bound Au that is still in some cationic state. If reduction does occur then there will be an immediate change in the absorption of the sample, turning from brown to a dark brown, red, or black color to indicate the formation of nanoparticles or aggregated neutral Au. If there is no reduction, indicating all protein-bound Au has already been reduced, then no nanoparticles or aggregate will be formed and there will be no observed change in the samples absorption. Transmission electron microscopy (TEM), confirms the existence of nanoparticles under the conditions that the absorbance of the BSA-Au + sodium borohydride sample is altered. This method does not directly prove the existence of a Au_{25} nanocluster, or any nanocluster, though it does prove the existence of protein-bound cationic gold, supporting the hypothesis that cationic gold is not reduced by aromatic residues. It is known that this partial reduction of cationic Au by tyrosine is possible at high pH, greater than 11.5, thus understanding weather red fluorescence is observed due to Au reduction or other factors is important.[53-54]

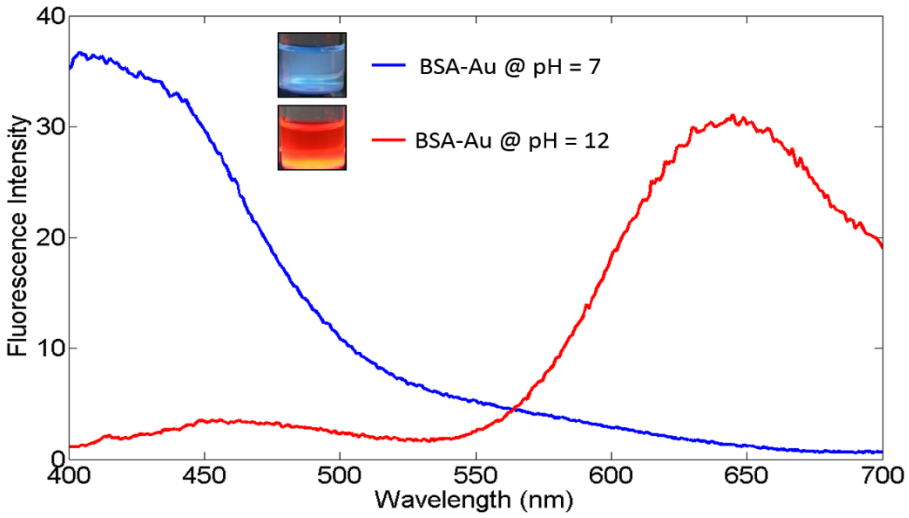

Figure 2. Fluorescence (λ_{ex} = 365 nm) of BSA-Au at pH = 7 and BSA-Au compound at pH = 12, the replicated sample first described by Xie et al.

The synthesis and subsequent red fluorescence of the BSA-Au compounds is highly dependent on the pH of the solution and this is shown in results where BSA-Au compounds synthesized and adjusted to neutral pH do not alter the intrinsic blue fluorescence (λ_{em} = 420 nm) of the protein when excited by λ_{ex} = 365 nm (**Figure 2**). BSA has five unique pH-induced conformational states at which the protein begins to unfold, two important conformational points are at pH 8 the 'basic' form and pH 10 the 'aged' form. If aromatic reduction is indeed the pathway in which red fluorescence emerges then fluorescence should begin at pH ~ 11.5, though if this fluorescence shift is due to conformational changes in the protein then fluorescence should occur at one of the five transitional pH points. By finely adjusting pH in the region around 8, 10, and 11.5, the pH-dependence can elucidated, confirming either a conformational induced wherein red fluorescence is directly related to the conformational state of the protein dictated by pH or is aromatic induced, where red fluorescence is related to the reducing potential of tyrosine and other aromatic

residues. These results would continue to support the hypothesis that this is a BSA-Au(III) complex and not a formed Au nanocluster.

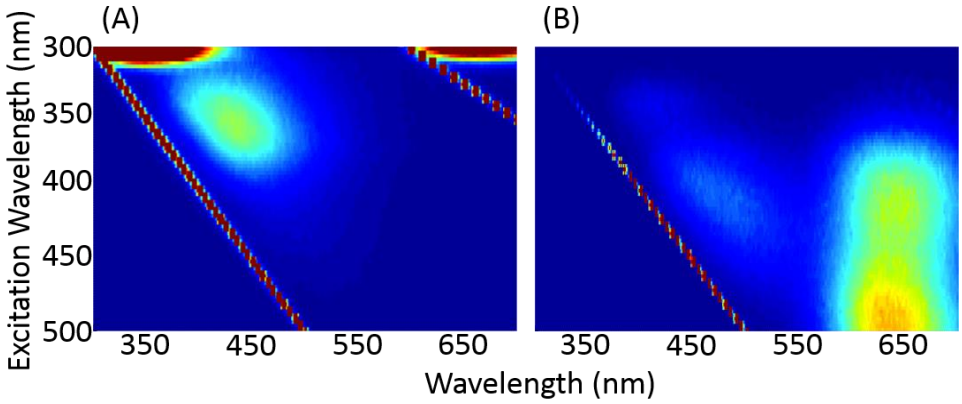

Figure 3. Excitation-emission map (excitation: 300-500 nm; emission: 300-700 nm) of (A) BSA at pH = 7 and (B) BSA-Au compound at pH = 12 both after 2 hours. These fluorescence maps indicate a possible energy transfer pathway as Au is introduced to BSA.

Formation of the red fluorophore is a slow process and little is currently known about the fluorescence mechanism. It takes approximately 2 hours for red fluorescence to be qualitatively observed under UV excitation and even over the course of multiple days the sample is observed to change color from yellow to dark yellow to brown. Time-course measurements by way of fluorescence spectroscopy could lend insight into the Au binding process and red fluorescence emergence (**Figure 3**). By using three-dimensional fluorescence excitation-emission maps instead of the conventional single excitation line scans, observed fluorescence could be analyzed according to a wider range of excitation wavelengths. Samples of the BSA-Au compound at different pH values and at different times in the synthesis (0, 2, 24, 48, and 96 hours) can be interpreted, and the Au binding process as well as the subsequent emergence of fluorescence can be elucidated.

In the original synthesis of the BSA-Au compound the addition of 1 mL of 10 mM $HAuCL_4$ to 1 mL of 0.751 mM (50 mg/mL) BSA has the stoichiometric ratio of BSA:Au

= 1:13.3, though it is stated that the Au(0) nanoclusters that are formed are Au_{25} nanoclusters. The adjustment of the $HAuCl_4$ concentration higher or lower in-turn will yield a different stoichiometric ratio between BSA and Au. This experimental design can lend insight into the amount of Au that is necessary to produce red fluorescence and could support the hypothesis that this fluorescence is indeed not a Au(0) nanocluster but is some BSA-Au compound. By adjusting the ratio of BSA to Au above and below the ratio of 1:13 and analyzing the point at which fluorescence emerges and subsequently peaks, could tell something about the mechanism of red fluorescence.

In order to gain insights into the binding location of Au, assuming the BSA-Au compound is not a neutral Au(0) nanocluster, various experimental approaches can be undertaken to elucidate these binding sites (**Figure 4**). It is known that serum albumins act as transport proteins[55] and as for BSA, the Asp-fragment is a known binding site at the N-terminus.[2-3] It has been previously reported that this N-terminus site chelates in square planer geometry Cu(II) and Ni(II)[56] and that the affinity for Cu(II) is higher than that of Ni(II).[57] This means that Cu(II) will compete with and replace Ni(II) if both are in solution. Though no such studies have been conducted about the binding of Au to this N-terminus site. Au(III) is also known to have a square planar geometry[58] like Cu(II) and Ni(II) and thus could potentially bind to the Asp-fragment. Assuming binding does occur then a similar competitive study using Cu(II) and Ni(II) could be deployed. Analyzing the results using absorption spectroscopy could tell weather Au(III) is replacing or is being replaced by each cation, respectively. Further data can be taken from this experiment as this binding site could be part of the mechanism of red fluorescence. If the fluorescence spectra is

altered when Au(III) can no longer bind to the Asp-fragment then this site could potentially be involved in red fluorescence generation.

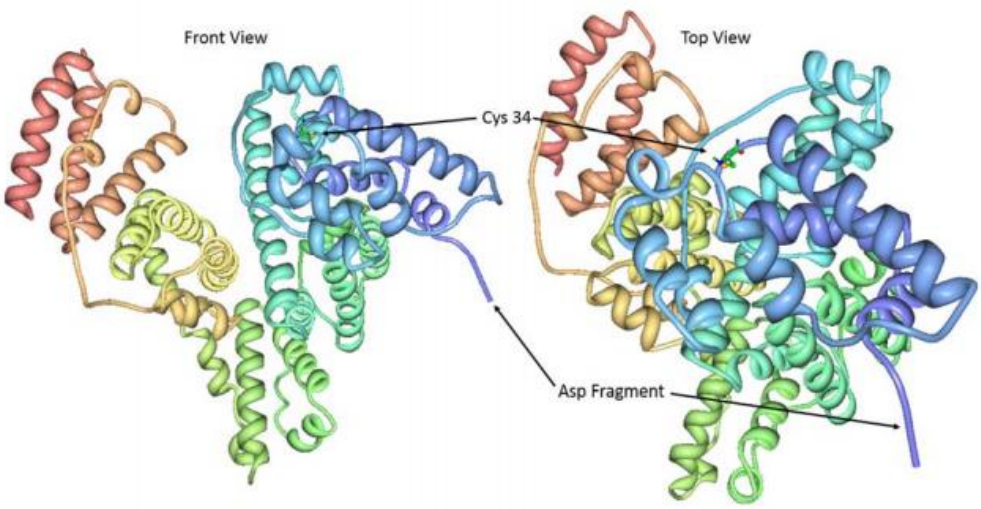

Figure 4. Crystal structure of BSA. The locations of cysteine 34 (Cys-34) and the Asparagine fragment are indicated. PDB-ID: 4F5S.

The synthesis procedure for these BSA-copper-gold (BSA-Cu(II)-Au(III)) and BSA-nickel-gold (BSA-Ni(II)-Au(III)) complexes is as follows: Synthesis using copper and nickel followed protocol (1) for BSA−Au(III). 0.5 mL of 20 mM CuCl2·2H2O or NiCl2·6H2O aqueous solution is added to 1 mL of aqueous BSA (0.75 mM) at 37 °C under vigorous stirring at 750 rpm. After 2 min, 1 M NaOH is added to achieve the pH of 12. The reaction proceeded for 2 h. Two hours after the formation of BSA−Cu(II) or BSA−Ni(II), 0.5 mL of HAuCl4 (20 mM) is added. After 2 min, 1 M NaOH is added to achieve the pH of 12. The reaction proceeded for 2 h, then the solution is stored at room temperature.

Further binding sites can also be elucidated by analyzing the effects of binding to the thiol groups of the cysteine clusters. It is well known that Au binds very strongly to thiol[59] and it is even proposed by others that the nucleation site of this Au_{25} nanocluster is internally bound inside the protein at one of these cysteine cluster locations.[1, 6, 33] Of the 35

cysteines in BSA, 34 are bound in disulfide configurations which can be grouped in 9 cysteine clusters.[2] Only one thiol - cysteine 34 (Cys-34) - is free to bind and is located on the surface of BSA and exposed in the proteins monomer form. By first adding a thiol capper, N-ethylmaleimide (NEM) and then reacting with Au, this free thiol can be removed as a binding site for Au. If this free Cys-34 is no longer available for binding and alters the fluorescence spectra of the BSA-Au compound then it can be elucidated as a part of the fluorescence mechanism.

The synthesis procedure to form this cysteine-34 capped complex ([Cys-34-capped] BSA-Au(III)) is as follows: Two mg of BSA is dissolved in 1 mL of phosphate buffered saline (PBS, pH 7.4), containing 2 mg of NEM. The solution is incubated at 20 °C with gentle stirring for 1 h. The solution is then dialyzed in PBS for 20 h to remove the excess NEM. 1.0 mL of HAuCl4 (0.4 mM) is then added to the solution and allowed to incubate for 2 min at 37 °C. 1 M NaOH is added to adjust the pH to 12, and the solution is incubated for 2 h at 37 °C under vigorous stirring.

Finally, many studies claim that the red fluorescence is due to Au nucleation at one of the 9 cysteine disulfide clusters.[1,6] In order to confirm the effects of thiol binding at any of the 35 cysteine residues, a complete capping of these thiols can be employed. Cysteines act as the backbone of BSA and other proteins and give them their tertiary structure; as such, these residues are usually buried inside the proteins hydrophobic pockets. In order to remove all cysteine thiols as potential binding sites the protein must first be partially unfolded, the disulfide bonds broken, and then all free thiols capped so that Au cannot interact with them. The proposed method to achieve this is to first slightly denature the protein using urea. Urea, is known to form hydrogen bonds with exposed amide-groups of

proteins backbones, inducing unfolding. Secondly, disulfides will be cut using tris(2-carboxyethyl)-phosphine hydrochloride (TCEP), exposing all thiols. Last, all free thiols will be permanently capped using NEM. It is known that Au reacts with the amine functional group of urea[60-61] and thus before reacting the newly capped BSA with Au, the solution will first be dialyzed to remove excess reactants. With all thiols capped Au will not be able to bind to any cysteine residues. If red fluorescence is not observed then it will indicate that at least one of the cysteine thiols are required for binding. Subsequent experimentation can then be conducted in order to locate the exact cysteine cluster or disulfide bond required for red fluorescence.

The procedure to synthesize these all thiol capped complexes ([all-thiol-capped-BSA]-Au(III) is as follows: One mL of BSA solution is prepared at 3.33 mg/mL in 2 M urea and 50 mM ammonium bicarbonate (NH_4HCO_3, pH 8.0). TCEP is added from a 0.25 M stock solution to a final concentration of 8 mM, and the solution is incubated for 1 h at 50 °C with gentle stirring. The solution is allowed to cool to 20 °C before NEM is added to a final concentration of 16 mM, and incubated for 2 h at room temperature. The solution is then dialyzed against 12−14 kDa membrane (DiaEasy, BioVision) in 50 mM NH_4HCO_3 to remove excess reactants. One mL of aqueous HAuCl4 (0.67 mM) is added at 37 °C under vigorous stirring. After 2 min, 1 M NaOH is added to bring the pH to 12 and the solution continued to incubate for 2 h at 37 °C under vigorous stirring.

CHAPTER 4: RESULTS

The as-synthesized BSA-Au compounds according to protocol (1), at pH =12 and 37°C reproduce the initially reported results of Xie et al.; fluorescing red when excited with UV (λ = 365 nm) (**Figure 5**). The color of the compound changed from clear to light yellow after adding Au to BSA, then from light yellow to dark yellow after 2 hours at 37°C, and finally from dark yellow to brown after 48 hours when stored at room temperature. The emergence of this red fluorescence was very slow, unable to be qualitatively detected until after an hour at 37°C and continued to slightly increase in intensity over the next 2 days when stored at room temperature. When preparing the BSA-Au compounds at a neutral pH of 7.0, the sample was a yellow-brown color and was blue fluorescent when excited under λ = 365 nm light (**Figure 2**).

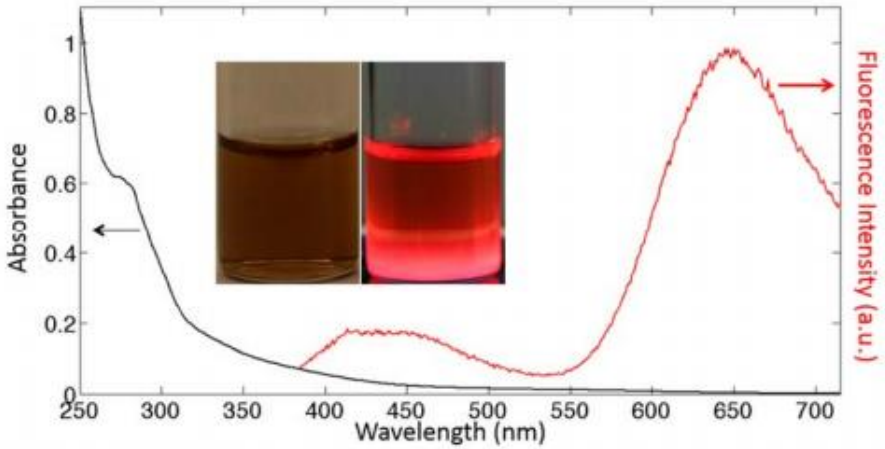

Figure 5. The compound of Xie *et al.* was reproduced according to protocol (1). The inset shows the brown color under ambient light and is red fluorescence when excited with UV ($\lambda_{ex}/\lambda_{em}$ = 365/645).

4.1 Reduction of the BSA-Au Complex

The BSA-Au compounds that were synthesized according to protocol (1) and at a range of final pH values were reduced after first dialyzing to remove excess reactants, and formed nanoparticles upon the addition of sodium borohydride shown by TEM imaging (**Figure 6**). The BSA-Au compounds were filtered using a 30 kDa cutoff-weight membrane, reducing the solution volume through centrifugation at 4000 rpm. Repeating this process multiple times removed the un-reacted and non-protein-bound cationic Au from solution. The reduction of the compound thus caused all remaining protein-bound Au to be reduced to Au(0). The reduced solutions all subsequently changed color upon addition of sodium borohydride and a surface plasmon peak at λ = 525 nm in each spectra is consistent with the formation of small nanoparticles of size around 5 nm (**Figure 7**).[37, 62] The BSA-Au compound prepared at a pH of 12 resulted in a wine-red colored solution, which indicates colloidal Au nanoparticles.[37] After reducing the BSA-Au compound prepared at pH 10 the sample resulted in a brown solution and the BSA-Au compound prepared at pH = 9 appeared light brown.

Analysis of the TEM images indicated that the size of the nanoparticles for the BSA-Au sample at pH 12 was 6.3 ± 2.9 nm; 3.3 ± 1.4 nm for the sample at pH = 10; and 1.6 ± 0.7 for BSA-Au prepared at pH = 9 as seen in **Figure 6**. While the formation of these nanoparticles does not directly disprove the existence of a neutral Au_{25} nanocluster in the BSA-Au compounds, it does confirm the existence of some protein-bound Au cations. Thus, these BSA-Au compounds can now more aptly be called BSA-Au(III) complexes, which follows similar nomenclature in studies of BSA metal-cation compounds.[3, 8-17] The formation of these nanoparticles of varying size related directly to the pH of the BSA-

Au(III) complex, this suggests different possible binding configurations of BSA to Au(III) inside the protein molecule. The initial report by Xie et al. and others[52] provide matrix assisted laser desorption-ionization time-of-flight (MALDI-TOF) measurements, reporting a peak at 71 kDa for BSA-Au and attributing the mass difference from BSA (66 kDa) as 25 Au atoms forming a neutral Au_{25} nanocluster.

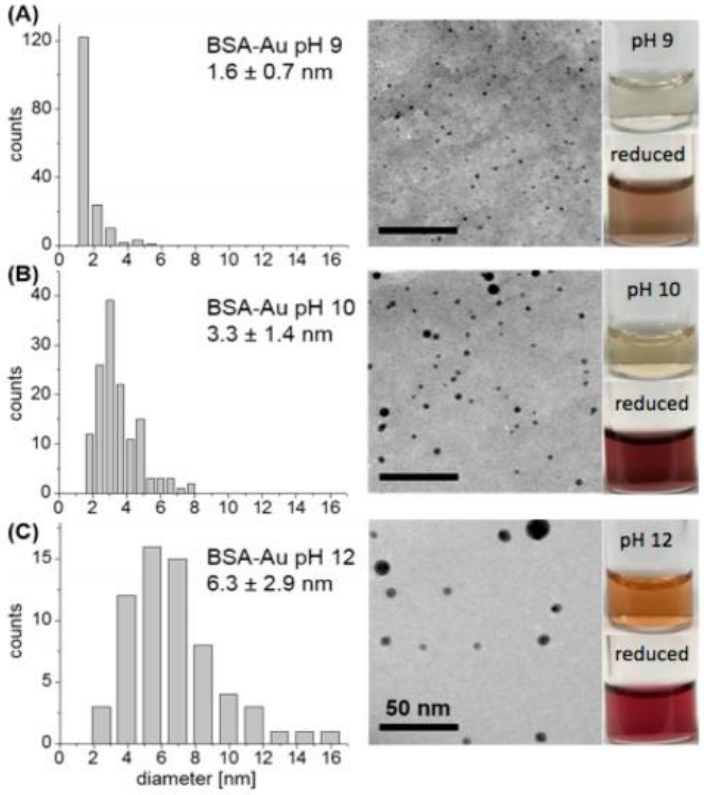

Figure 6. Nanoparticles formed by reducing BSA−Au(III) complexes that were synthesized at (A) pH = 9, (B) pH = 10, and (C) pH = 12. The histograms and the transmission electron microscopy (TEM) images indicate different incorporation of Au(III) with BSA, thus resulting in different size distributions. The BSA−Au(III) complexes under ambient light are light yellow (pH = 9), light orange (pH = 10), and light brown (pH = 12), respectively. The nanoparticles of the BSA−Au(III) at pH = 12 shows a wine red color, which is an indication of the formation of colloidal nanoparticles. Reduced BSA−Au (III) at pH = 9 and 10 are light brown and dark brown, respectively.

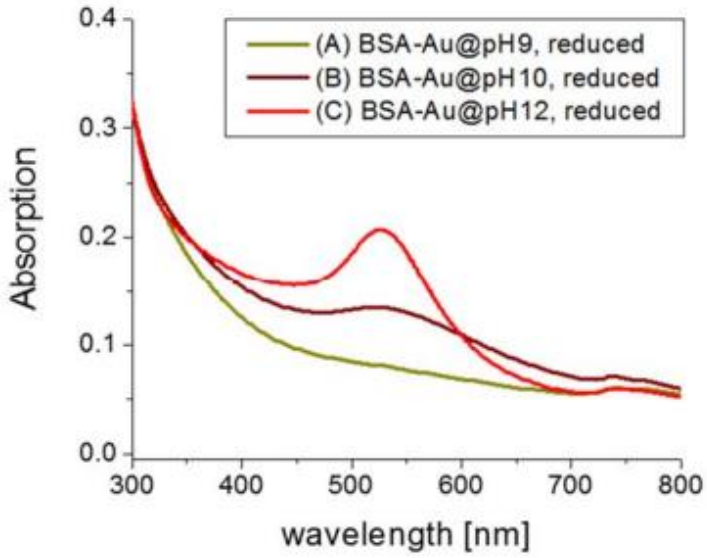

Figure 7. The absorbance of BSA-Au synthesized according to protocol (1) at pH = 9, 10, 12, and then reduced using NaBH4. The absorption spectra show surface plasmon peaks at λ = 520 nm for the reduced BSA-Au at pH=10 and 12. This is consistent with the formation of nanoparticles of size ~5 nm observed by transmission electron microscopy in Figure 6. The absorption line-shape is also consistent with small (< 2 nm) nanoparticle formation for pH = 9.

4.2 Fluorescence of BSA-Au Complex and BSA Conformation

In order to elucidate the pH-dependence of the red fluorescence in the BSA-Au(III) complexes, the pH was finely adjusted, following protocol (1). The pH was altered from neutral to basic in order to determine the threshold at which red fluorescence occurs. Based on our results, the threshold for red fluorescence emergence is at pH = 9.7 ± 0.2 (**Figure 8**). As the pH of the BSA-Au(III) complex was finely increased from 9.0 to 10.5, the blue fluorescence ($\lambda_{ex}/\lambda_{em}$ = 365/440 nm) decreased and the red fluorescence ($\lambda_{ex}/\lambda_{em}$ = 365/640 nm) proportionally increased (**Figure 9**). The fluorescence of the solution also appeared a violet color, indicating the existence of both blue fluorescing and red fluorescing species simultaneously. BSA is known to have a pH-induced conformational transition from its B-form (basic-form, ~8 < pH < ~10), to its A-form (aged-form, pH > ~10) at around pH =

9.6.[2, 63] At this pH transition point, an equilibrium is reached where BSA is in both B-form and A-form equally. This observation, where the change in fluorescence color is gradual and not instantaneous strongly suggests that the red fluorescence in the BSA-Au(III) complex is due to the conformational state of the protein molecule, sterically determining available binding sites for Au(III), and not due to the reduction of BSA by tyrosine and the other 46 aromatic residues.

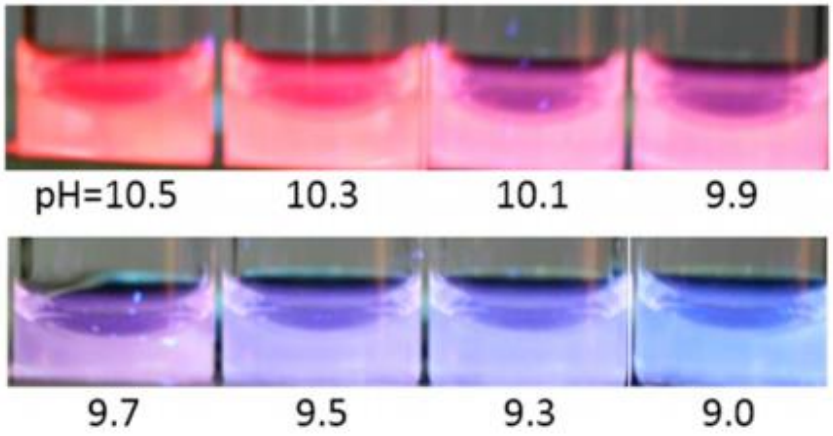

Figure 8. Fluorescence (λ_{ex} = 365 nm) of BSA−Au(III) synthesized around pH = 10. The threshold of the emergence of red fluorescence is around pH = 9.7 ± 0.2.

This transition point at the pH of 9.7 ± 0.2 indicates that the hydroxyl group (the group responsible for reduction) is not at a high enough pK_a (pK_{aR} = 11.5) to reduce the gold from Au(III) to Au(0) as was previously suggested.[1] This is a secondary evidence supporting the hypothesis that a formation BSA-Au(III) is being made, rather than a neutral Au(0) nanocluster. Further analysis of the pH-adjusted BSA-Au(III) (**Figure 9**) shows an isosbestic point at around 570 nm, indicating a conversion of the blue-fluorescing BSA in B-form to the red-fluorescing species in A-form. This is consistent with the pH-induced conformational change of the protein.

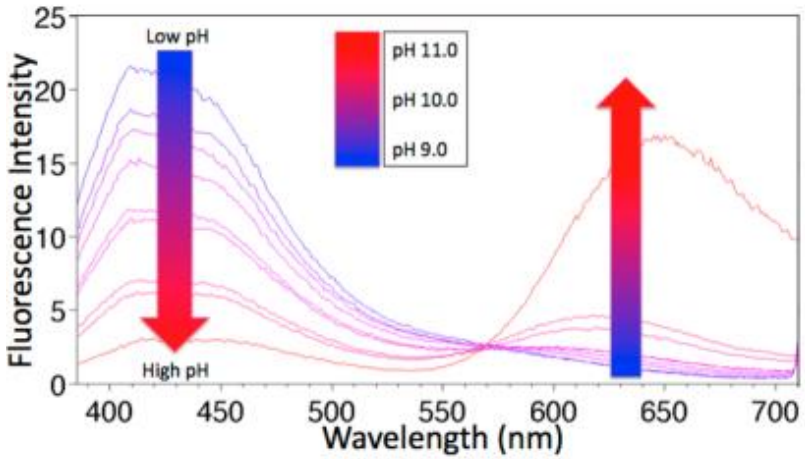

Figure 9. Fluorescence line scans (λ_{ex} = 365 nm) of BSA−Au(III) complexes synthesized at various pH. The isosbestic point at λ_{em} = 570 nm indicates the conversion of a blue-fluorescent species into a red-fluorescent species as the pH is increased.

4.3 Au to BSA Binding Process

In order to understand the mechanism of the Au(III) binding process to BSA, in relation to the conformation of BSA, we analyzed the time-course of the BSA-Au(III) complex using excitation-emission mapping of the fluorescence. These excitation-emission maps (EE-maps) of BSA and BSA-Au(III) at pH =7 and BSA-Au(III) at pH = 12 allow us to observe the fluorescence in a larger array of excitation wavelengths as opposed to single-line excitation scans in the literature. Using these EE-maps we can observe the change in fluorescence according to the pH and the addition of Au(III) to BSA (**Figure 10**). All EE-maps will have linear excitation streaks (Rayleigh line) with intensities as well as their second-order harmonics due to the excitation wavelength being detected at the same emission wavelength. The intrinsic UV fluorescence of BSA alone at pH = 7 (λ_{ex}/ λ_{em} = 290/340 nm, 'UV peak') in its natural N-form is due to the two tryptophan residues inside the protein.[33, 63-64] This N-form also has another fluorescence peak that can be seen in the EE-map when exciting at λ = 340 nm and emitting at λ = 420 nm, this 'blue peak' is also

due to the other 64 aromatic residues according to their local environments,[65] although the overall mechanism of this fluorescence is not found in other literature. As BSA moves from its natural conformational N-form to the more open and detangled A-form, due to pH activated unfolding, changes in the protein's tertiary structure around the aromatic residues leads to a change in the fluorescence map. Thus in the EE-map of BSA at pH =12 a peak is found again when exciting at λ = 340 nm and emitting at λ = 420 nm, but the peak is more drawn out towards the longer wavelengths.

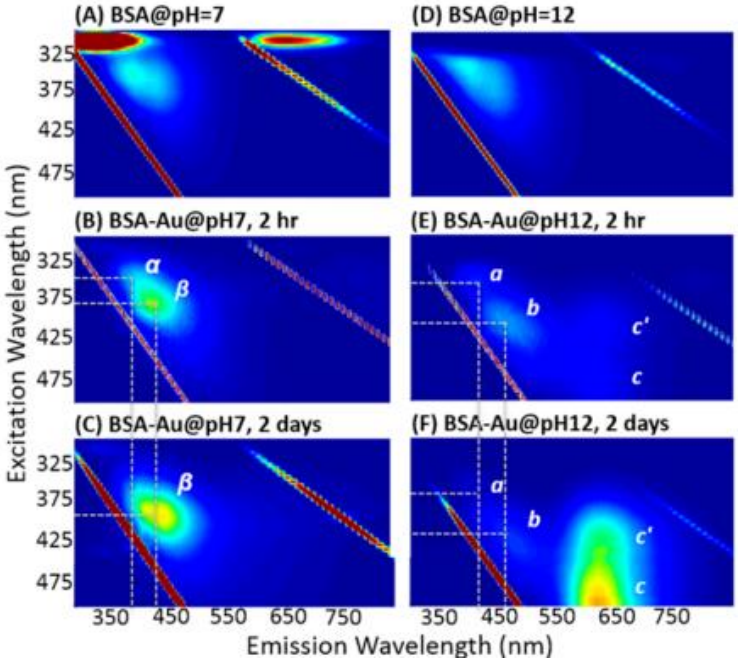

Figure 10. Time-course of the excitation−emission map (excitation: 290−500 nm; emission: 300−850 nm) of BSA and BSA−Au(III) complexes at pH = 7 and 12. For BSA at pH = 7, (A) BSA at pH = 7 (N-form BSA), (B) BSA−Au at pH = 7, 2 hours after synthesis, and (C) BSA−Au@pH = 7, 48 hours after synthesis. For BSA at pH = 12, (D) BSA at pH = 12 (A-form BSA), (E) BSA− Au at pH = 12, 2 hours after synthesis, (F) BSA−Au at pH = 12, 48 hours after synthesis. The letter insets in panels B and C indicate, α: $\lambda_{ex}/\lambda_{em}$ = 350/ 380 nm; β: $\lambda_{ex}/\lambda_{em}$ = 380/420 nm. The letter insets in panels E and F indicate, a: $\lambda_{ex}/\lambda_{em}$ = 370/400 nm; b: $\lambda_{ex}/\lambda_{em}$ = 400/460 nm; c′: $\lambda_{ex}/\lambda_{em}$ = 400/640 nm; c: $\lambda_{ex}/\lambda_{em}$ = 470/640 nm. These indicate possible enrgy transfer pathways from a → b, b → c', and b → c.

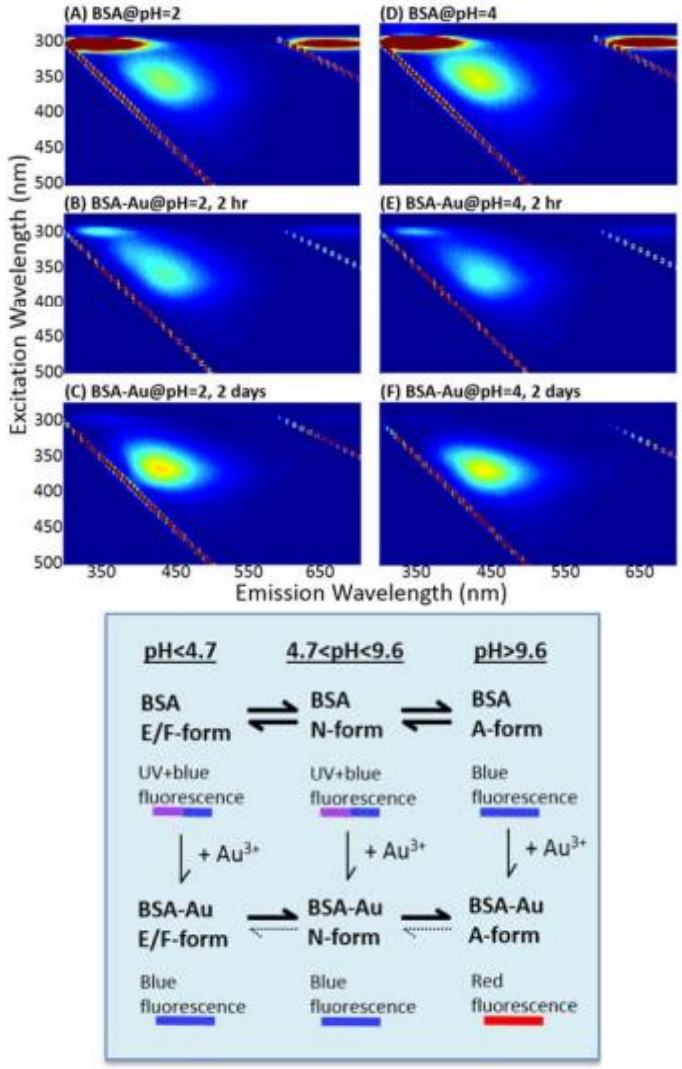

Figure 11. Top Image: Time-course of the excitation-emission map (excitation: 275 – 500 nm; emission: 300 – 700 nm) of BSA and BSA-Au(III) complexes at pH = 2 and 4. (A) BSA at pH=2 (E-form BSA), (B) BSA-Au at pH=2, 2 hours after synthesis, (C) BSA-Au at pH=2, 48 hours after synthesis. (D) BSA at pH = 4 (F-form BSA), (E) BSA-Au at pH=4, 2 hours after synthesis, (F) BSA-Au at pH=4, 48 hours after synthesis. The time-course of both samples at pH = 2 and pH = 4 is essentially identical to that of BSA at pH=7 and BSA-Au at pH=7. BSA-Au at pH=2 and BSA-Au at pH=4 showed no color under ambient light. Bottom Image: A qualitative summary of the relation between pH and the fluorescence of BSA and BSA-Au. The red fluorescence of BSA-Au at pH=12 was found to be stable over weeks in neutral (pH = 7) as well as in acidic (pH = 4) conditions. On the other hand, when BSA-Au at pH = 4 and at pH = 7 were put into basic (pH = 12), they exhibited red fluorescence within a few hours.

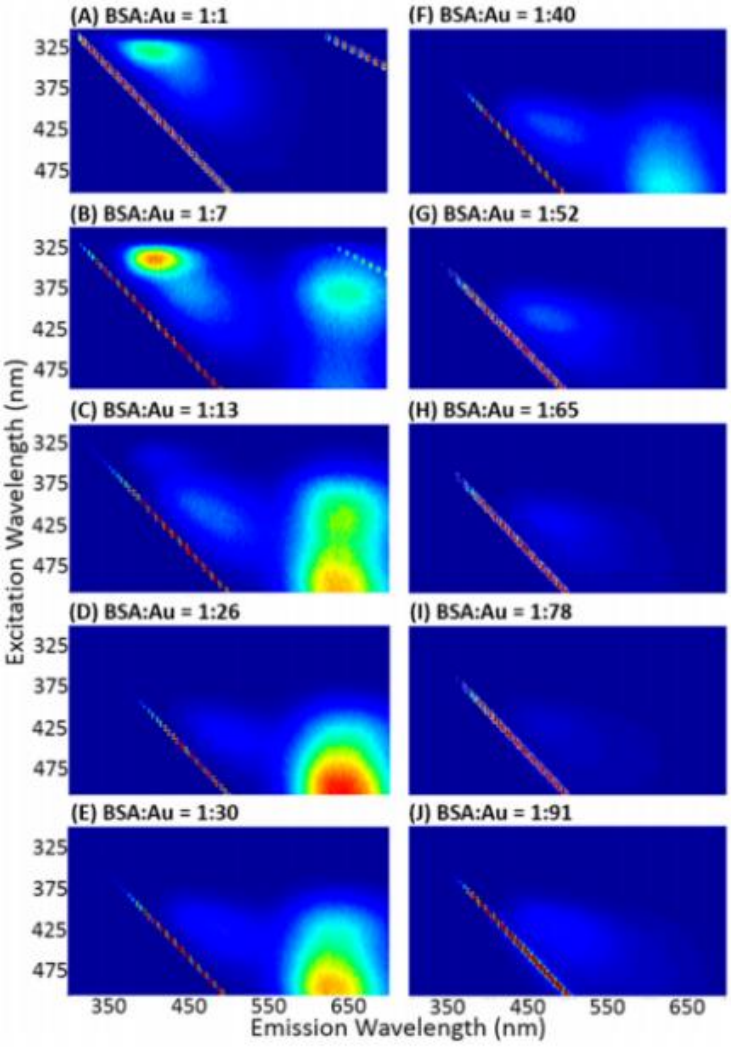

Figure 12. Ratiometric studies of the BSA−Au(III) complexes at pH = 12, 48 hours after synthesis. Excitation−emission maps (excitation: 300−500 nm; emission: 300−700 nm) for the BSA:Au stoichiometric ratios of (A) 1:1, (B) 1:7, (C) 1:13, (D) 1:26, (E) 1:30, (F) 1:40, (G) 1:52, (H) 1:65, (I) 1:78, (J) 1:91.

The emergence of different fluorescence peaks was studied after the addition of Au(III) at two time points: 2 hours after synthesis at 37^{o}C and 2 days after synthesis at 20^{o}C. In the BSA-Au complex synthesized at pH = 7, the 'UV peak' was suppressed significantly at 2 hours. The interpretation of these peaks in the EE-maps can assume an energy transfer between the peak at $\lambda_{ex}/\lambda_{em}$ = 350/380 nm (peak α), and the peak at $\lambda_{ex}/\lambda_{em}$

= 350/420 nm (peak β). Analyzing the time-course shows a slight red-shift in both the excitation and emission. Time-course EE-maps of BSA-Au(III) at pH =2 (E-form) and pH = 4 (F-form) are nearly identical to that of BSA-Au(III) in N-form (**Figure 11**).

Adding Au(III) caused a large shift of the BSA fluorescence as can be seen in the EE-map of BSA-Au(III) at pH = 12 compared to BSA alone. These peaks can also be well understood assuming an energy-transfer mechanism. It can be seen that the peaks at $\lambda_{ex}/\lambda_{em}$ = 370/400 nm (peak *a*); 400/460 nm (peak *b*); 400/640 nm (peak *c'*); 470/640 nm (peak *c*) suggest the possible energy transfer pathways: $a \rightarrow b$, $a \rightarrow c'$, and $b \rightarrow c$. Slight red-shifting of the fluorescence in both excitation and emission are found in these time-course measurements as well. The multiple peaks found in these EE-maps indicate a feasible cascade energy transfer, where-by energy transfer from peak *a* and *b* excites the chromophore corresponding to both peak *c* and *c*'. Thus it is possible to hypothesize multiple chromophores and/or multiple binding sites of Au(III) in the protein.

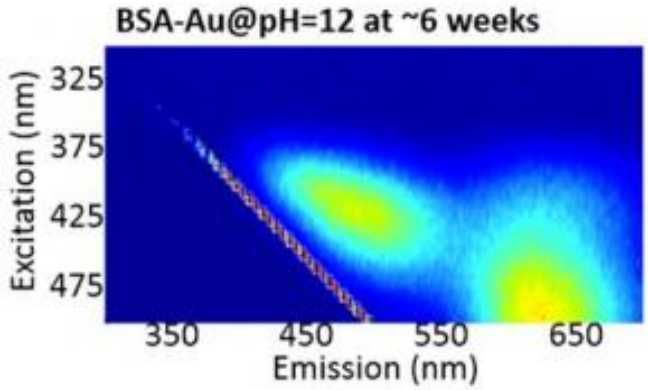

Figure 13. Excitation-emission map of BSA-Au@pH=12 (BSA:Au stoichiometric ratio of 1:13), 6 weeks after synthesis.

By changing the BSA-to-Au molar ratio, it may lead to elucidating the Au(III) binding process. In the original synthesis by Xie et al. and others the ratio of BSA-to-Au

is 1 : 13. Thus, following the synthesis protocol (1), outlined in the methods, the ratio of BSA-to-Au was varied between 1 : 1 and 1 : 100. After synthesis the fluorescence of the samples was characterized after 48 hours using a 'ratio-metric EE-map' (**Figure 12**).

Overall, there are motifs between the time-course EE-map and the ratio-metric EE-map in **Figure 11**. There are identical excitation and emission peaks in the two measurement sets. We also observed the ratio-metric EE-map of BSA : Au = 1 : 26 at 48 hours was virtually identical to an aged sample of BSA : Au = 1 : 13 at 6 weeks (**Figure 13**). This suggests that the time-course of fluorescence emergence is a slow process of incorporating Au(III) into the protein. The reason for this slow incorporation, which happens on the order of days, is due to the slow conformational change of BSA into its A-form.[2] The slow incorporation may also be due to the coordination sphere of $AuCl_4^-$ changing to $Au(OH)_4^-$ upon the pH change from neutral to 12. It has been shown that the coordination of Au(III) cations are much less liable compared to Cl^- anions[66] and thus, a lesser amount of Au(III) are available to be incorporated into BSA. Considering this, the ratio-metric results obtained are consistent with a decrease in fluorescence for BSA-Au(III) complexes when prepared according to protocol (2), where the pH of the $HAuCl_4$ solution is first pre-adjusted to pH = 12 and then added to the BSA solution (**Figure 14**).

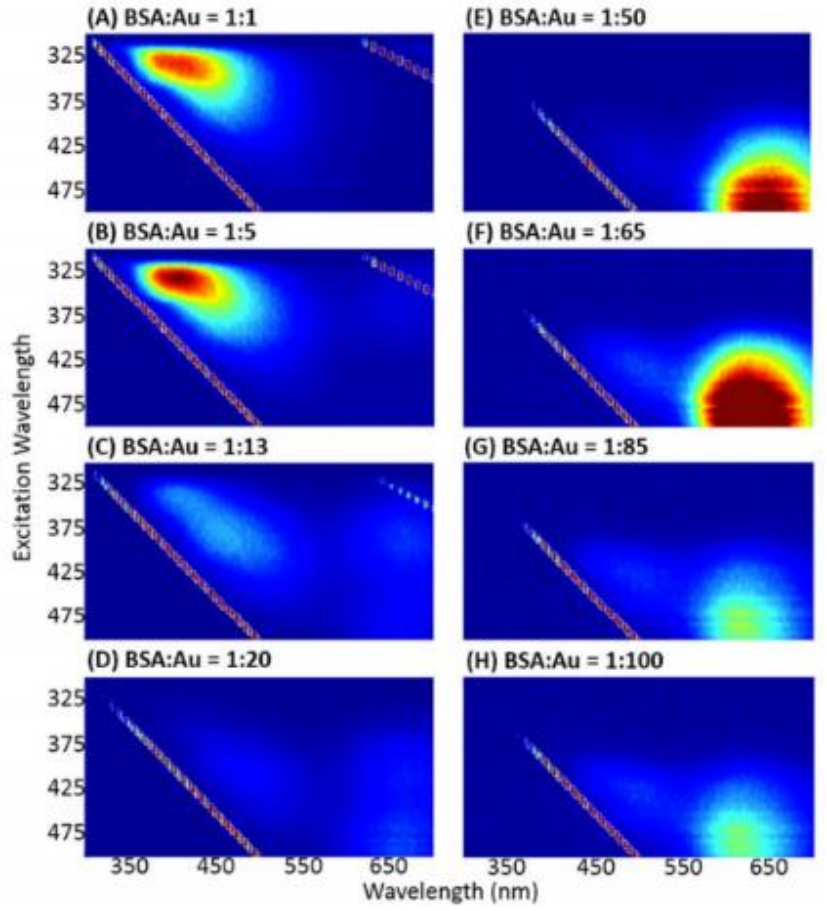

Figure 14. Ratiometric studies of the BSA-Au(III) complexes prepared according to protocol (2), where the pH of BSA solution and $HAuCl_4$ was pre-adjusted to 12, then mixed. Excitation-emission maps (excitation: 300 – 500 nm; emission: 300 – 700 nm) for the BSA:Au stoichiometric ratios of (A) 1:1, (B) 1:5, (C) 1:13, (D) 1:20, (E) 1:50, (F) 1:65, (G) 1:85, (H) 1:100.

For the molar ratio of BSA : Au = 1 : 1, no red fluorescence was detected and the EE-map showed the same fluorescence pattern as that of BSA alone at pH = 12. Though, red fluorescence was observed for the molar ratio of 1 : 7, even though the total average number of Au(III) to BSA was almost 4 times less than 25. When Au(III) was added in excess, above a molar of 1 : 30, the red fluorescence slowly diminished and was quenched beyond a molar ratio of 1 : 52. Thus, the maximum number of Au(III) that can be incorporated into BSA is less than 30 Au(III) per BSA in ensemble average. However, the

minimum number of Au(III) required to produce red fluorescence is less than 7, but may be more than 1. It is also noted that there is a slow and gradual emergence of fluorescence which begins when excited with λ = 365 nm light, at lower ratios and shifts to lower energy excitation at λ = 495 nm when the BSA-to-Au ratio is high. This shifting in the maximum fluorescence peak approximately obeys[67] $h\nu \sim E_F N^{-1/3}$, where E_F is the Fermi energy of bulk Au and N is the number of gold atoms, which is expected from 25 neutral Au atoms nucleating at a single site to form a Au_{25} nanocluster. This relationship was not observed in either the time-course or ratio-metric EE-maps.

4.4 Au Binding Site – Asparagine Fragment

In order to gain insights into the binding site or sites of Au(III) in BSA, we used previously-studied systems of BSA-Cu(II)[3, 8, 11] and BSA-Ni(II)[9-10] complexes (**Figure 15**). It is known that both Cu(II) and Ni(II) have a single binding site in BSA N-form, when the protein is at neutral pH = 7. This binding site known as the 'Asp-fragment' is the first 3 amino acid residues exposed at the N-terminus of BSA. It is also known that the affinity of Cu(II) to the Asp-fragment site, via chelation by square-planar geometry is stronger than that of Ni(II). Therefore, when Cu(II) and Ni(II) both competitively bind to the Asp-fragment Cu(II) will replace Ni(II).[57] There may be more binding sites for Cu(II) and Ni(II), in addition to the Asp-fragment, when BSA is in it's a-form at pH = 12; however, additional binding sites have not been found by others. Au(III), like Cu(II) and Ni(II) also predominately has a square-planar geometry.[68] Thus, by adding in Au(III) to an already-synthesized BSA-Cu(II) or BSA-Ni(II) complex, one can determine whether one of three interactions occurs. The first interaction is that Au(III) interacts with the Asp-fragment like

Cu(II) and Ni(II) and displaces them, secondly, Au(III) interacts with another site, or finally, Au(III) reacts with both the Asp-fragment and another binding site.

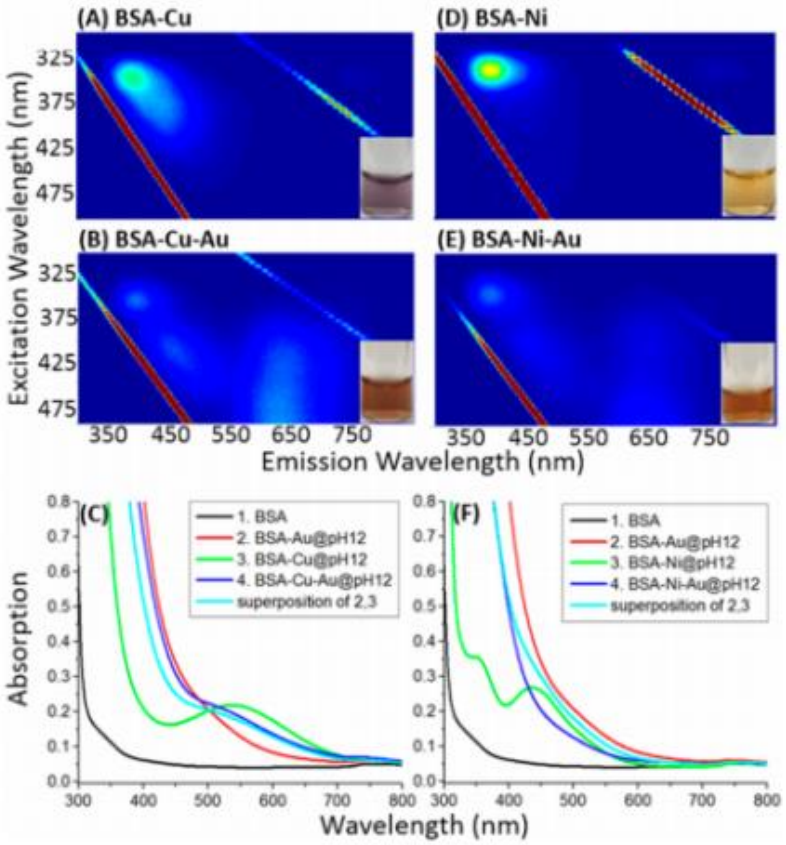

Figure 15. Excitation−emission maps (excitation: 290−500 nm; emission: 300−850 nm) of (A and D) BSA complexed with Cu(II)/ Ni(II) at pH = 12, (B and E) BSA complexed with Cu(II)/Ni(II) and then with Au(III) at pH = 12, (C and F) absorption spectra comparing (1) BSA; (2) BSA−Au; (3) BSA−Cu(II)/Ni(II); and (4) BSA−Cu(II)/ Ni(II)−Au(III). Curve 4 is compared with the superposition of Curves 2 and 3.

When synthesizing BSA-Cu(II) complexes at pH = 12 the sample was a bright purple under ambient light and BSA-Ni(II) at pH = 12 was a dark yellow under ambient light. This can be seen in the insets of **Figure 15**, and represents the chelation of Cu(II) and Ni(II) to the Asp-fragment. The EE-maps of both BSA-Cu(II) and BSA-Ni(II) were virtually similar to that of BSA at pH = 12. It is note though, that the overall fluorescence intensities of all peaks was much lower than those of BSA-alone. This overall fluorescence

quenching when BSA is in the presence of metal cations (specifically when there is non-specific binding to the proteins surface) has also been reported by others.[69] These results indicate that the Asp-fragment does not contribute to the intrinsic fluorescence of BSA and that Cu(II) along with Ni(II) both suppress the 'UV peak' and 'blue peak' specific to BSA.

The BSA-Cu(II) and BSA-Ni(II) complexes were allowed to mix for two hours before the addition of Au(III). Two hours after the addition of Au(III), both complexes lost their original purple and yellow color from BSA-Cu(II) and BSA-Ni(II), respectively. This suggests that there was an incorporation of Au(II) into BSA. By comparing the absorption spectra before and after the addition of Au(III) into BSA-Cu(II) and BSA-Ni(II), it was found that Cu(II) had remained bounded to the Asp-fragment while Ni(II) was replaced by Au(III) at the site (**Figure 15**). Therefore it can be said that the Asp-fragment is a weak biding site for Au(III), but the characteristic red fluorescence of BSA-Au(III) is not located at this site as both samples of BSA-Cu(II)-Au(III) and BSA-Ni(II)-Au(III) still displayed the red fluorescence. The conversion of the 'blue peak' and the emergence of the red peak was similar to BSA-Au(III) at pH = 12 without the addition of Cu(II) or Ni(II). These observation indicate that while the Asp-fragment is a biding site for Au(III), it is not involved in the red fluorescence generation and there is more than one binding site for Au(III) in BSA.

4.5 Au Binding Site – Cysteine Thiols

It is well known that Au(III) has a strong affinity for the thiol functional group and the strongest among all metals (Au > Ag > Cu > Ni > Pt).[70-71] Thus, Au(III) can bind to any thiol site, including the surface-accessible single-free thiol (Cys34) and one or many of the other 17 Cys-Cys disulfide bonds that make up to backbone of BSA tertiary structure.

Binding to these sites is dependent on their steric accessibility for Au(III) and biding preference may be different between each thiol group. With this in mind, one can illustrate the involvement of cysteine residues and their thiol functional group in the BSA-Au(III) complex formation by eliminating Au-thiol bonding from in the protein.

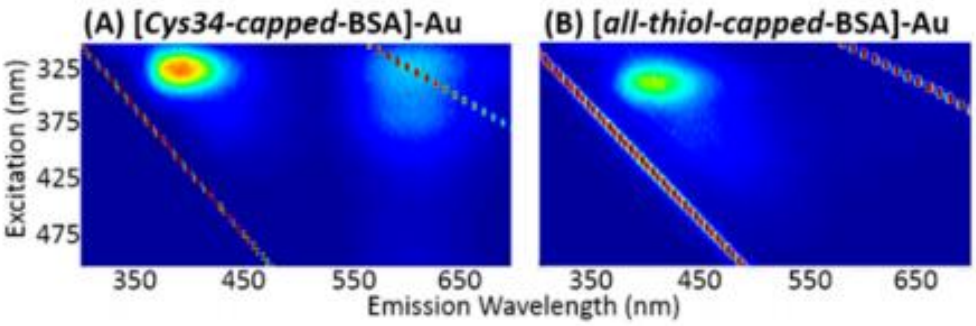

Figure 16. Excitation−emission map (excitation: 300−500 nm; emission: 300−700 nm) of (A), Cys34-capped BSA reacted with Au at pH = 12 and (B), all Cys−Cys disulfide bonds in BSA cleaved and capped then the all-thiol-capped-BSA was reacted with Au at pH = 12.

First, it is easier to determine binding to the free cysteine thiol (Cys34) which is surface-accessible at all pH conditions. Thus, we capped the thiol of Cys34 by using N-ethylmaleimide (NEM) according to a standard protocol[72] and dialyzed the sample. Then used the dialyzed, Cys34-capped BSA to react with Au(III). Due to the high affinity of Au for thiol, it is expected that the Au(III) binds to the Cys34 or will bind to the still surface-accessible Cys34-Cys34 disulfide bond in the case of a BSA dimer. Though, the exact ratio of BSA monomer to dimer used in this experiment is not known. This binding of Au to Cys34 has also been explored by others.[19, 73] The EE-map of a Cys43-capped-BSA-Au(III) can be seen in **Figure 16**. However, when comparing the red-fluorescence peak in the EE-map of Cys43-capped-BSA-Au(III) to that of just BSA-Au(III) the peak at $\lambda_{ex}/\lambda_{em}$ = 350/ 640 nm was dimmer compared to the peaks of *c'* and *c* as in **Figure 10**. Thus, it can be

seen that Cys34 is a Au(III) binding site, but does not affect the generation of red fluorescence and is as-such, not the location of the red fluorophore. These results are consistent with BSA-Au(III) at pH = 7 where BSA is in its N-form and still has the surface-accessible Cys34, which does not yield red fluorescence. It is possible, but yet unconfirmed, that Au(III) bound to the Cys34 site is involved in the energy transfer mechanism, based on the alteration of the EE-map of Cys43-capped-BSA-Au(III). The absence of Au(III) at this binding site may result in an inefficient excitation of the red fluorophore.

In order to elucidate one of the 17 disulfide bonds as red fluorophore site we cleaved all the cysteine-cysteine bonds in BSA using a standard protocol.[72, 74] By using 2 M urea and tris(2-carboxyethyl)-phosphine (TCEP) in order to open the protein and cut the disulfide bonds, the resulting 34 free thiols, as well as Cys34, was capped using NEM and finally dialyzed to remove any excess reactants. This all-thiol-capped-BSA ('linearized BSA') was then reacted with Au(III) to produce a linearized-BSA-Au(III) complex. This complex did not show any red fluorescence and these observations demonstrate that either one of the 17 disulfide bonds or one of the 34 disulfide-bound thiols is required for red fluorescence (**Figure 16)**.

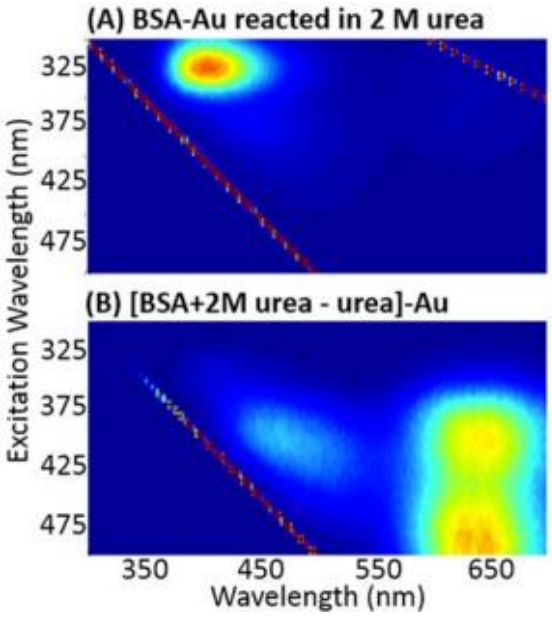

Figure 17. Effect of urea in the reaction of BSA and Au. Urea is used to denature BSA (while Cys-Cys disulfide bonds are preserved), to enable the disulfide bond cleaving by TCEP according to standard procedure (A) BSA reacted with HAuCl4 according to protocol (1) at pH = 12 (BSA:Au stoichiometric ratio of 1 : 13) in the presence of 2 M urea did not yield red-fluorescent compound. (B) BSA was treated with 2 M urea, then dialyzed to remove the urea. The dialyzed BSA was reacted with HAuCl4 according to protocol (1) at pH = 12. This yielded the same red fluorescent BSA-Au compound without the urea processing, resulting in a similar E-E map. We thus confirmed the successful removal of urea by dialysis.

It is important to note that urea is a strong detergent and forms hydrogen bonds with the surface-exposed amide-groups of protein backbones; this induces unfolding of the protein and exposes the buried disulfide bonds. BSA, when reacted with Au(III) in 2 M urea showed no red fluorescence (**Figure 17**), due to the reaction of Au(III) to the amine functional groups of urea.[61, 75] To ensure that the addition and subsequent dialysis of urea did not affect the Au(III) binding in **Figure 16**, a control experiment was performed where BSA was incubated with 2 M urea. After incubating for 2 hours in 2 M urea, the BSA-urea solution was dialyzed overnight to remove the urea. BSA is a dynamic and resilient protein, and is known to refold to its natural conformation after being perturbed from equilibrium.[2]

Thus this ‘BSA + urea – urea’ solution was reacted with Au(III) following the original protocol (1) with a BSA-to-Au ratio of 1 : 13 and yielded the exact same red fluorescence as BSA-Au(III) at pH = 12 (**Figure 10**) when comparing the EE-maps.

CHAPTER 5: DISCUSSION

For a consistent description of all the experimental observations, we hypothesize that Au(III) atoms coordinate to one of 17 cysteine-cysteine disulfide bond sites, which alters the intrinsic blue fluorescence of aromatic amino acid residues to red fluorescence. Specifically, there are nine cysteine clusters found in BSA[2, 76] and are as follows (**Figure 18**): **Site I**: Cys53-Cys62, consisting of one single cys-cys disulfide bond, and eight other cys-cys disulfide bond pairs; **Site II**: Cys75−Cys91 and Cys90−Cys101; **Site III**: Cys123−Cys168 and Cys167−Cys176; **Site IV**: Cys199−Cys245 and Cys244−Cys252; **Site V**: Cys264−Cys278 and Cys277−Cys288; **Site VI**: Cys315−Cys360 and Cys359−Cys368; **Site VII**: Cys391−Cys437 and Cys436−Cys447; **Site VIII**: Cys460−Cys476 and Cys475−Cys486, and finally; **Site IX**: Cys513−Cys558 and Cys557−Cys566.

In previous X-ray crystallographic studies on apo-ferritin from horse liver, Au(III) was found to bind to cysteine, as well as methionine and histidine residues,[77-79] but neutral Au(0) nanoparticles were only formed under reduction by addition of $NaBH_4$.[77] The presence of methionine and histidine residues (thioether sulfur and imidazole nitrogens, respectively) in the vicinity of a cysteine-cysteine disulfide bond in the tertiary structure may further stabilize the Au(III) binding.[77-82] In the N-form of BSA (BSA at pH = 7), all the cysteine-cysteine bonds are enclosed in hydrophobic pockets, buried in the protein and are inaccessible by Au(III).

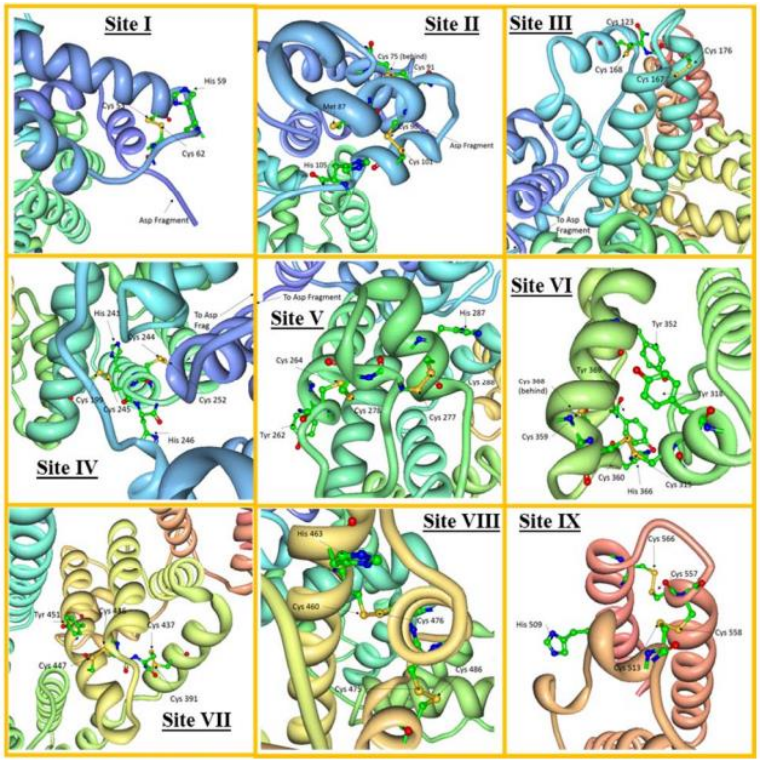

Figure 18. Cys-Cys disulfide bond sites (Site I – IX) in BSA.

After a conformational change induced by pH from N-form to A-form at pH = 9.6, some cys-cys disulfide bonds are expected to be sufficiently exposed and solvent-accessible. The alpha-helix percentages of BSA in N-form are 55 % and 48 % in A-form.[2, 63] It is noted that the X-ray crystallographic data is only available for BSA in N-form,[76] and is not available in A-form. Though, it is feasible to assume that BSA in it's A-form is more disentangled than in its N-form, and all cysteine-cysteine bonds and all cysteine-cysteine loops will remain intact at all experimental conditions, including pH ($3 < pH < 12$) and temperature ($T < 50^{o}C$). Upon further inspection for residues aromatic residues that are close the cysteine-cysteine bonds; **Site I**: Has a His59 on the cys-cys loop and is only 7.9 Å away; **Site II**: Has a His105 and Met87 close but outside of the cys-cys loop; **Site IV**: His241, which is 7.1 Å away, on the loop and His246 outside the loop; **Site V**:

Has Tyr262 outside the loop and His287, close to and inside the loop; **Site VI**: His366 is close (6.3 Å on the loop), with Tyr318 and Tyr369 outside the loop; **Site VII**: Has a single Tyr451 outside the loop, and lastly; **Site VIII**: His463 is close to the cys-cys disulfide bond (5.7 Å) and is on the loop (**Figure 18**). All these cysteine-cysteine cluster sites are favorable Au(III) binding sites for red fluorescence.

In regards to the existence internal energy transfer pathways in the BSA-Au(III) complex at pH = 12, Au(III) may bind to one or more cysteine-cysteine sites among **Sites I-IX**, in addition to the non-fluorophore-forming Cys34 and Asp-fragment sites. Multiple Au(III) binding sites, both strong and weak, has been suggested by others.[83-84] Thus, a plausible origin of the red fluorophore could involve, ligand field (LF), ligand-to-metal charge transfer (LMCT), and/or metal-to-ligand charge transfer (MLCT) transitions,[85-91] although more details are still needed about the local coordination at the cysteine-cysteine disulfide bond sites in order to fully elucidate the red florescence mechanism. Additionally, a strong electron delocalization could occur at one or many aromatic residues, amongst at least one of the nine cys-cys sites (**Sites I-IX**), for example via dehydration or cyclization.[92-94] However, it has yet to be determined if such processes can be arbitrated by Au(III).

CHAPTER 6: CONCLUSIONS

To summarize all the experimental findings, the red fluorescence in BSA-Au(III) complexes emerges due to Au cations combining with BSA at or above a pH = 9.7 ± 0.2. The threshold for red fluorescence in the BSA-Au(III) complexes coincides with the reversible isomeric transitions, induced by pH change, of BSA into its A-form and is not induced by aromatic residue reduction, which requires a pH greater than pH = 11.5. These as-synthesized BSA-Au(III) complexes were further reducible upon the addition of a chemical reducing agent – $NaBH_4$ – and formed neutral Au nanoparticles in excess reductant. It was also determined that, the emergence of red fluorescence was a slow process, taking more than 48 hours for fluorescence to maximize at 20^{o}C. Gradual red shifting of the fluorescence wavelength, which is expected for Au(0) nanocluster nucleation at one bind site in BSA, based on the spherical Jellium model, was not observed. The ensemble minimum number of Au(III) per BSA required to yield red fluorescence was found to be more than 1 and less than 7. The UV-excitable red fluorescence of the BSA-Au(III) complex ($\lambda_{ex}/\lambda_{em}$ = 350/ 640 nm) is due to the internal, and possible cascaded, energy transfers among one or multiple chromophores in BSA. From the above observations, we concluded that the synthesized compound is not a neutral Au_{25} nanocluster, and is instead, an uncharacterized metal-protein complex of BSA-Au(III). It has been found that there is not one, but multiple specific binding sites for Au(III) in BSA these include: (1) the Asp-fragment located at the N-terminus of BSA, (2) Cys34, a free

surface-bound cysteine thiol, and (3) one or many solvent-accessible cysteine-cysteine disulfide bonds in BSAs A-form, but not in N-form.

The elucidation of the red fluorophore and the mechanism that drives fluorescence would be of large relevance to protein and bioinorganic chemistry, in addition to nanoscience. The determination of the exact Au(III) binding sites ultimately requires crystallographic studies of BSA complexed with Au(III) in both its N-form and A-form, however protein crystallization studies involving bound metals at extreme pH values is currently very difficult.[76, 95] Controlled enzymatic fragmentations could provide information on the local Au(III) interaction with the cysteine-cysteine disulfide bonds and aromatic amino acid residues. Thus, it may be possible to elucidate a smaller amino acid sequence in BSA which contains the red fluorophore and it may lend insight into the exact cysteine-cysteine clusters that bind Au(III) and generate red fluorescence.

REFERENCES

1. Xie, J.; Zheng, Y.; Ying, J. Y., Protein-Directed Synthesis of Highly Fluorescent Gold Nanoparticles. *J. Am. Chem. Soc.* **2009,** *131*, 888-889.

2. Peters, T., Jr, *All About Albumin*. 1996.

3. Peters, T., Jr; Blumenstock, F. A., Copper-Binding Properties of Bovine Serum Albumin and Its Amino-terminal Peptide Fragment. *J. Biol. Chem.* **1967,** *242*, 1574-1578.

4. Sadler, P. J.; Tucker, A., pH-induced structural transitions of bovine serum albumin: Histidine pKa values and unfolding of the N-terminus during the N to F transition. *European Journal of Biochemistry* **1993,** *212*, 811-817.

5. Zheng, J.; Zhang, C.; Dickson, R. M., Highly Fluorescent, Water-Soluble, Size-Tunable Gold Quantum Dots. *Phys. Rev. Lett.* **2004,** *93* (7).

6. Qu, X.; Li, Y.; Li, L.; Wang, Y.; Liang, J.; Liang, J., Fluorescent Gold Nanoclusters: Synthesis and Recent Biological Application. *J. Nanomater.* **2015,** (784097).

7. Chen, L.-Y.; Wang, C.-W.; Yuan, Z.; Chang, H.-T., Fluorescent Gold Nanoclusters: Recent Advances in Sensing and Imaging. *Anal. Chem.* **2015,** *87* (1), 216-229.

8. Klotz, I. M.; Curme, H. G., The Thermodynamics of Metallo-protein Combinations. Copper with Bovine Serum Albumin. *J. Am. Chem. Soc.* **1948,** *70*, 939-943.

9. Fiess, H. A.; Klotz, I. M., The Thermodynamics of Metallo—Protein Combinations. Comparison of Copper Complexes with Natural Proteins. *J. Am. Chem. Soc.* **1952,** *74*, 887-891.

10. Rao, M. S. N., A Study of the Interaction of Nickel(II) with Bovine Serum Albumin. *J. Am. Chem. Soc.* **1962,** *84*, 1788-1790.

11. Fiess, H. A., The Interaction of Cobalt with Native Proteins. *J. Am. Chem. Soc.* **1952,** *74*, 3539-3541.

12. Liu, H. y.; Xu, Z. h.; Liu, X. h.; Xi, P. x.; Zeng, Z. z., Analysis of Binding Interaction between Bovine Serum Albumin and the Cobalt(II) Complex with Salicylaldehyde-2-phenylquinoline-4- carboylhydrazone. *Chem. Pharm. Bull.* **2009,** *57*, 1237-1242.

13. Masuoka, J.; Saltman, P., Zinc(II) and Copper(II) Binding to Serum Albumin. A Comparative Study of Dog, Bovine, and Human Albumin. *J. Biol. Chem.* **1994,** *269*, 25567-25561.
14. Ohyoshi, E.; Hamada, Y.; Nakata, K.; Kohata, S., The interaction between human and bovine serum albumin and zinc studied by a competitive spectrophotometry. *J. Inorg. Bio.* **1999,** *75*, 213-218.

15. Shears, G. E.; Ledward, D. A.; Neale, R. J., Iron Complexation to Carboxyl Groups in a Bovine Serum Albumin Digest. *International J. of Food Science and Technology* **1987,** *22*, 265-272.

16. Ueno, H. M.; Urazono, H.; Kobayashi, T., Serum Albumin fFrms a Lactoferrin-like Soluble Iron-Binding Complex in Presence of Hydrogen Carbonate Ions. *Food Chemistry* **2014,** *145*, 90-94.

17. Irons, L. I.; Perkins, D. J., Studies on the Interaction of Magnesium, Calcium and Strontium Ions with Native and Chemically Modified Human Serum Albumin. *Biochem.* **1962,** *84*, 152-156.

18. Lakatos, B.; Szentmihályi, K.; Vinkler, P.; Balla, J.; Balla, G., The role of essential metal ions in the human organism and their oral supplementation to the human body in deficiency states. *Orv Hetil.* **2004,** *145* (25), 1315-1319.

19. Bal, W.; Sokołowska, M.; Kurowska, E.; Faller, P., Binding of transition metal ions to albumin: Sites, affinities and rates. *Biochimica et Biophysica Acta* **2013,** *1830*, 5444-5455.

20. Saito, M.; Arakaki, R.; Yamada, A.; Tsunematsu, T.; Kudo, Y.; Ishimaru, N., Molecular Mechanisms of Nickel Allergy. *Int J Mol Sci.* **2016,** *17* (2), 202.

21. Patel, S. U.; Sadler, P. J.; Tucker, A.; Viles, J. H., Direct detection of albumin in human blood plasma by proton NMR spectroscopy. Complexation of nickel2+. *J. Am. Chem. Soc.* **1993,** *115* (20), 9285-9286.

22. Simonsen, L. O.; Harbak, H.; Bennekou, P., Cobalt metabolism and toxicology—A brief update. *Science of The Total Environment* **2012,** *432*, 210-215.

23. Carter, E. L.; Flugga, N.; Boer, J. L.; Mulrooneya, S. B.; Hausinger, R. P., Interplay of metal ions and urease. *Metallomics* **2009,** (3), 177-268.

24. Mothes, E.; Faller, P., Evidence that the Principal CoII-Binding Site in Human Serum Albumin Is Not at the N-Terminus: Implication on the Albumin Cobalt Binding Test for Detecting Myocardial Ischemia. *Biochemistry* **2007,** *46* (8), 2267-2274.

25. Sokołowska, M.; Wszelaka-Rylik, M.; Poznańskib, J.; Bal, W., Spectroscopic and thermodynamic determination of three distinct binding sites for Co(II) ions in human serum albumin. *Journal of Inorganic Biochemistry* **2009,** *103* (7), 1005-1013.

26. Stewart, A. J.; Blindauer, C. A.; Berezenko, S.; Sleep, D.; Sadler, P. J., Interdomain zinc site on human albumin. *PNAS* **2003,** *100* (7), 3701-3706.

27. Bal, W.; Christodoulou, J.; Sadler, P. J.; Tucker, A., Multi-metal binding site of serum albumin. *Journal of Inorganic Biochemistry* **1998,** *70* (1), 33-39.

28. Fanali, G.; Cao, Y.; Ascenzi, P.; Fasano, M., Mn(II) binding to human serum albumin: A 1H-NMR relaxometric study. *Journal of Inorganic Biochemistry* **2012,** *117*, 198-203.

29. Sheftel, A. D.; Mason, A. B.; Ponk, P., The long history of iron in the Universe and in health and disease. *Biochimica et Biophysica Acta (BBA)* **2012,** *1820* (3), 161-187.

30. McKie, A. T.; Marciani, P.; Rolfs, A.; Brennan, K.; Wehr, K.; Barrow, D.; Miret, S.; Bomford, A.; Peters, T. J.; Farzaneh, F.; Hediger, M. A.; Hentze, M. W.; Simpson, R. J., A Novel Duodenal Iron-Regulated Transporter, IREG1, Implicated in the Basolateral Transfer of Iron to the Circulation. *Molecular Cell* **2000,** *5* (2), 299-309.

31. Silva, A. M. N.; Hider, R. C., Influence of non-enzymatic post-translation modifications on the ability of human serum albumin to bind iron: Implications for non-transferrin-bound iron speciation. *Biochimica et Biophysica Acta (BBA)* **2009,** *1794* (10), 1449-1458.

32. Tong, J.-Q.; Tian, F.-F.; Li, Q.; Li, L.-L.; Xiang, C.; Liu, Y.; Dai, J.; Jiang, F.-L., Probing the Adverse Temperature Dependence in the Static Fluorescence Quenching of BSA Induced by a Novel Anticancer Hydrazone. *Photochem. Photobio. Sci.* **2012,** *11*, 1868-1879.

33. Russell, B. A.; Kubiak-Ossowska, K.; Mulheran, P. A.; Birch, D. J. S.; Chen, Y., Locating the Nucleation Sites for Protein Encapsulated Gold Nanoclusters: A Molecular Dynamics and Fluorescence Study. *Phys. Chem. Chem. Phys.* **2015,** *17*, 21935-21941.

34. Kang, X.; Chong, H.; Zhu, M., Au25(SR)18: The Captain of the Great Nanocluster Ship. *Nanoscale* **2018,** *10* (23), 10758-10834

35. Schaaff, T. G.; Knight, G.; Shafigullin, M. N.; Borkman, R. F.; Whetten, R. L., Isolation and Selected Properties of a 10.4 kDa Gold:Glutathione Cluster Compound. *J. Phys. Chem. B* **1998,** *102* (52), 10643-10646.

36. Heaven, M. W.; Dass, A.; White, P. S.; Holt, K. M.; Murray, R. W., Crystal Structure of the Gold Nanoparticle [N(C8H17)4][Au25(SCH2CH2Ph)18]. *J. Am. Chem. Soc.* **2008,** *130* (12), 3754-3755.

37. Brust, M.; Walker, M.; Bethell, D.; Schiffrin, D. J.; Whyman, R., Synthesis of thiol-derivatised gold nanoparticles in a two-phase Liquid–Liquid system. *Journal of the Chemical Society* **1994,** *0* (0), 801-802.

38. Hostetler, M. J.; Green, S. J.; Stokes, J. J.; Murray, R. W., Monolayers in Three Dimensions: Synthesis and Electrochemistry of ω-Functionalized Alkanethiolate-Stabilized Gold Cluster Compounds. *J. Am. Chem. Soc.* **1996,** *118* (17), 4212–4213.

39. Mirkin, C. A.; Letsinger, R. L.; Mucic, R. C.; Storhoff, J. J., A DNA-based method for rationally assembling nanoparticles into macroscopic materials. *Nature* **1996,** *1* (382), 607-609.

40. Jin, R.; Wu, G.; Li, Z.; Mirkin, C. A.; Schatz, G. C., What Controls the Melting Properties of DNA-Linked Gold Nanoparticle Assemblies? *J. Am. Chem. Soc.* **2003,** *125* (6), 1643-1654.

41. Zhu, M.; Aikens, C. M.; Hollander, F. J.; Schatz, G. C.; Jin, R., Correlating the Crystal Structure of A Thiol-Protected Au25 Cluster and Optical Properties. *J. Am. Chem. Soc.* **2008,** *130* (18), 5883-5885.

42. Takano, S.; Yamazoe, S.; Koyasu, K.; Tsukuda, T., Slow-Reduction Synthesis of a Thiolate-Protected One-Dimensional Gold Cluster Showing an Intense Near-Infrared Absorption. *J. Am. Chem. Soc.* **2015,** *137* (22), 7027-7030.

43. Donkers, R. L.; Lee, D.; Murray, R. W., Synthesis and Isolation of the Molecule-like Cluster Au38(PhCH2CH2S)24. *Langmuir* **2004,** *20* (5), 1945-1952.

44. Zhu, M.; Lanni, E.; Garg, N.; Bier, M. E.; Jin, R., Kinetically Controlled, High-Yield Synthesis of Au25 Clusters. *J. Am. Chem. Soc.* **2008,** *130* (4), 1138-1139.

45. Parker, J. F.; Weaver, J. E. F.; McCallum, F.; Fields-Zinna, C. A.; Murray, R. W., Synthesis of Monodisperse [Oct4N+][Au25(SR)18−] Nanoparticles, with Some Mechanistic Observations. *Langmuir* **2010,** *26* (16), 13650-13654.

46. Xie, J.; Lee, J. Y.; Wang, D. I. C.; Ting, Y. P., Silver Nanoplates: From Biological to Biomimetic Synthesis. *ACS Nano* **2007,** *1* (5), 429-439.

47. Yu, L.; Banerjee, I. A.; Matsui, H., Direct Growth of Shape-Controlled Nanocrystals on Nanotubes via Biological Recognition. *J. Am. Chem. Soc.* **2003,** *125* (48), 14837-14840.

48. RR, N.; SJ, S.; G, A.; SE, J.; MO, S., Biomimetic synthesis and patterning of silver nanoparticles. *Nat. Mater.* **2002,** *1* (3), 169-172.

49. Ignatenko, A. V.; Cherenkevich, S. N.; Komyak, A. I., Chromatographic and spectroscopic investigation of the products of oxidation of tyrosine with ozone. *Journal of Applied Spectroscopy* **1984,** *41* (1), 798-802.

50. Xue, Y.; Li, X.; Li, H.; Zhang, W., Quantifying thiol–gold interactions towards the efficient strength control. *Nature Communications* **2014,** *1* (5), 43-48.

51. Pensa, E.; Cortés, E.; Corthey, G.; Carro, P.; Vericat, C.; Fonticelli, M. H.; Benítez, G.; Rubert, A. A.; Salvarezza, R. C., The Chemistry of the Sulfur–Gold Interface: In Search of a Unified Model. *Acc. Chem. Res.* **2012,** *45* (8), 1183-1192.

52. Guével, X. L.; Hotzer, B.; Jung, G.; Hollemeyer, K.; Trouillet, V.; Schneider, M., Formation of Fluorescent Metal (Au, Ag) Nanoclusters Capped in Bovine Serum Albumin Followed by Fluorescence and Spectroscopy. *J. Phys. Chem. C* **2011,** *115*, 10955-10963.

53. Cha, S.-H.; Kim, J.-U.; Kim, K.-H.; Lee, J.-C., Preparation and Photoluminescent Properties of Gold(I)−Alkanethiolate Complexes Having Highly Ordered Supramolecular Structures. *Chem. Mater.* **2007,** *19* (25), 6297-6303.

54. Maruyama, T.; Fujimoto, Y.; Maekawa, T., Synthesis of gold nanoparticles using various amino acids. *J. Colloid Interface Sci.* **2015,** *447* (1), 254-257.

55. Kragh-Hansen, U., Molecular Aspects of Ligand Binding to Serum Albumin. *Pharmacol Rev.* **1981,** *33* (1), 17-53.

56. Theodore Peters, J.; Blumenstock, F. A., Copper-binding Properties of Bovine Serum Albumin and Its Amino-terminal Peptide Fragment. *J. Biol. Chem.* **1966,** *242* (7), 1574-1578.

57. Kolthoff, I. M.; B. R. Willeford, J., The Interaction of Copper(II) with Bovine Serum Albumin. *J. Am. Chem. Soc.* **1958,** *80* (21), 5673-5678.

58. W. Roy Mason, I. H. B. G., Electronic Structures and Spectra of Square-Planar Gold(III) Complexes. *Inorg. Chem.* **1967,** *7* (1), 55-58.

59. Xue, Y.; Li, X.; Li, H.; Zhang, W., Quantifying Thiol–Gold Interactions towards the Efficient Strength Control. *Nat. Commun.* **2014,** *5*, 4348.

60. Sadeek, S. A.; Refat, M. S., Synthesis, Infrared Spectra and Thermal Investigation of Gold(III) and Zinc(II) Urea Complexes. *J. Coord. Chem.* **2005,** *58* (18), 1727-1734.

61. Egusa, S.; Ebrahem, Q.; Mahfouz, R. Z.; Saunthararajah, Y., Ligand Exchange on Gold Nanoparticles for Drug Delivery and Enhanced Therapeutic Index Evaluated in Acute Myeloid Leukemia Models. *Exp. Bio. Med.* **2014,** *239*, 853.

62. Lin, X.-M.; Sorensen, C. M.; Klabunde, K. J., *J. Nanopart. Res.* **2000,** *2* (157).

63. Theodore Peters, J., Serum Albumin. *Advances in Protein Chemistry* **1985,** *37* (1), 161-245.

64. JT, V.; PR, C., Mechanisms of tryptophan fluorescence shifts in proteins. *Biophys J.* **2001,** *80* (5), 2093-2109.

65. Lakowicz, J. R., *Principles of Fluorescence Spectroscopy, 3rd ed.* Springer: 1999.

66. Pacławski, K.; Zając, D. A.; Borowiec, M.; Kapusta, C.; Fitzner, K., EXAFS Studies on the Reaction of Gold (III) Chloride Complex Ions with Sodium Hydroxide and Glucose. *J. Phys. Chem. A* **2010,** *114* (44), 11943-11947.

67. J, Z.; PR, N.; RM, D., Highly fluorescent noble-metal quantum dots. *Annu Rev Phys Chem.* **2007,** *58*, 409-431.

68. Cotton, F. A.; Wilkinson, G., *Advanced Inorganic Chemistry*. Wiley-Interscience: New York, 1999.

69. Crouse, H. F.; Potoma, J.; Nejrabi, F.; Snyder, D. L.; Chohan, B. S., Quenching of tryptophan fluorescence in various proteins by a series of small nickel complexes. *Dalton Transactions* **2012,** *41* (9), 2720-2731.

70. Petrovykh, D. Y.; Kimura-Suda, H.; Opdahl, A.; Richter, L. J.; Tarlov, M. J.; Whitman, L. J., Alkanethiols on Platinum: Multicomponent Self-Assembled Monolayers. *Langmuir* **2006,** *22* (6), 2578-2587.

71. Ulman, A., Formation and Structure of Self-Assembled Monolayers. *Chem. Rev.* **1996,** *96* (4), 1533-1554.

72. Hermanson, G. T., *Bioconjugate Techniques, 3rd ed.* Acedemic Press: New York, 2013.

73. Christodoulou, J.; Sadler, P. J.; Tucker, A., A New Structural Transition of Serum Albumin Dependent on the State of Cys34. *Eur. J. Biochem.* **1994,** *225* (1), 363-368.

74. Giansanti, P.; Tsiatsiani, L.; Low, T. Y.; Heck, A. J. R., Six alternative proteases for mass spectrometry–based proteomics beyond trypsin. *Nature Protocols* **2016,** *11* (1), 993-1006.

75. Sadeek, S. A.; Refat, M. S., Synthesis, infrared spectra and thermal investigation of gold(III) and zinc(II) urea complexes. A new procedure for the synthesis of basic zinc carbonate. *J. Coord. Chem.* **2006,** *58* (18), 1727-1734.

76. Majorek, K. A.; Porebski, P. J.; Dayal, A.; Zimmerman, M. D.; Jablonska, K.; Stewart, A. J.; Chruszcz, M.; Minor, W., Structural and immunologic characterization of bovine, horse, and rabbit serum albumins. *Molecular Immunology* **2012,** *52* (4), 174-182.

77. Suzuki, M.; Abe, M.; Ueno, T.; Abe, S.; Goto, T.; Toda, Y.; Akita, T.; Yamadae, Y.; Watanabe, Y., Preparation and catalytic reaction of Au/Pd bimetallic nanoparticles in Apo-ferritin. *Chem. Commun.* **2009,** *0* (32), 4871-4873.

78. Künzle, M.; Lach, M.; Beck, T., Crystalline protein scaffolds as a defined environment for the synthesis of bioinorganic materials *Nat. Commun.* **2018,** *47* (31), 10382-10387.

79. Maity, B.; Abe, S.; Ueno, T., Observation of gold sub-nanocluster nucleation within a crystalline protein cage. *Nat. Commun.* **2017,** *0* (8), 14820.

80. Warżajtis, B.; Glišić, B. Đ.; Savić, N. D.; Pavic, A.; Vojnovic, S.; Veselinović, A.; Nikodinovic-Runic, J.; Rychlewska, U.; Djuran, M. I., Mononuclear gold(III) complexes with L-histidine-containing dipeptides: tuning the structural and biological properties by variation of the N-terminal amino acid and counter anion. *Dalton Transactions* **2017,** *46* (8), 2594-2608.

81. Wienken, M.; Lippert, B.; Zangrando, E.; Randaccio, L., Gold(III) glycyl-L-histidine dipeptide complexes. Preparation and x-ray structures of monomeric and cyclic tetrameric species. *Inorg. Chem.* **1992,** *31* (11), 1983-1985.

82. Best, S. L.; Chattopadhyay, T. K.; Djuran, M. I.; Palmer, R. A.; Sadler, P. J.; Sóvágó, I.; Varnagy, K., Gold(III) and palladium(II) complexes ofglycylglycyl-L-histidine: crystal structures of[AuIII(Gly-Gly-L-His-H-2)]Cl·H2O and[PdII(Gly-Gly-L-His-H-2)]·1.5H2O and HisεNH deprotonation. *Journal of the Chemical Society, Dalton Transactions* **1997,** *0* (15), 2587-2596.

83. Corbierre, M. K.; Lennox, R. B., Preparation of Thiol-Capped Gold Nanoparticles by Chemical Reduction of Soluble Au(I)−Thiolates. *Chem. Mater.* **2005,** *17* (23), 5691-5696.

84. III, C. F. S.; Schaeffer, N. A.; Elder, R. C.; Eidsness, K.; Trooster, J.; Calis, G. M., Bovine Serum Albumin-Gold Thiomalate Complex: 197Au Mossbauer, EXAFS and XANES, Electrophoresis, 35S-Radiotracer, and Fluorescent Probe Competition Studies. *J. Am. Chem. Soc.* **1984,** *0* (106), 3511-3521.

85. Lever, A. P. B., *Inorganic electronic spectroscopy, 2nd ed.* Elsevier: Amsterdam, 1984; Vol. I.

86. Eichhorn, G. L., *Inorganic Biochemistry*. Elsevier 1: Amsterdam, 1973.

87. Kaim, W.; Schwederski, B.; Klein, A., *Bioinorganic Chemistry -- Inorganic Elements in the Chemistry of Life: An Introduction and Guide, 2nd Ed.* Wiley: Chichester, 1994.

88. McMillin, D. R.; Morris, M. C., Further perspectives on the charge transfer transitions of blue copper proteins and the ligand moieties in stellacyanin. *Proc Natl Acad Sci U S A.* **1981,** *78* (11), 6567-6570.

89. Zawadzki, H. J., Synthesis and spectral studies of gold(III) complexes with guanidine derivatives. *Transition Metal Chemistry* **2003,** *28* (7), 820-826.

90. Gangopadhayay, A. K.; Chakravorty, A., Charge Transfer Spectra of some Gold(III) Complexes. *J. Chem. Phys.* **1961,** *0* (35), 2206.

91. Gray, H. B.; Ballhausen, C. J., A Molecular Orbital Theory for Square Planar Metal Complexes. *J. Am. Chem. Soc.* **1963,** *85* (3), 260-265.

92. Tubbs, J. L.; Tainer, J. A.; Getzoff, E. D., Crystallographic Structures of Discosoma Red Fluorescent Protein with Immature and Mature Chromophores: Linking Peptide Bond Trans−Cis Isomerization and Acylimine Formation in Chromophore Maturation. *Biochemistry* **2005,** *44* (29), 9833-9840.

93. Tsien, R. Y., The Green Fluorescent Protein. *Annual Review of Biochemistry* **1998,** *67*, 509-544.

94. O.Shimomura, Structure of the chromophore of Aequorea green fluorescent protein. *FEBS Letters* **1979,** *104* (2), 220-222.

95. McPherson, A.; Cudney, B., Optimization of crystallization conditions for biological macromolecules. *Acta Crystallogr F Struct Biol Commun.* **2014,** *70* (11), 1445-1467.